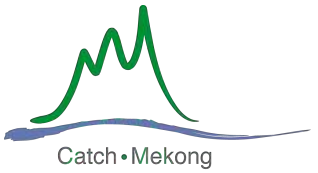

Master Thesis

Analysing Spatio-temporal Patterns of Coastal Aquaculture Based on Three Decades of Satellite Data

Dorothee Stiller

Matriculation Number: 1251887

Global Change Ecology (M.Sc.)

University of Bayreuth

First Supervisor:
Dr. Martin Wegmann
University of Würzburg

Second Supervisor:
Dr. Claudia Künzer
German Aerospace Center

In cooperation with: Dr. Patrick Leinenkugel, German Aerospace Center

February 2018

Legal Statement

Hiermit versichere ich, Dorothee Stiller, dass ich die vorliegende Arbeit selbstständig und unter Angabe aller Hilfsmittel und Referenzen angefertigt habe. Des Weiteren versichere ich, dass diese Arbeit in dieser oder ähnlicher Form noch keiner anderen Prüfungsbehörde vorgelegt wurde.

I, Dorothee Stiller, hereby declare that, to the best of my knowledge, this work does not bear resemblance to any other work in the whole or in part and has been completed myself. I did not use any other sources and means than specified. Furthermore, this work has not been previously submitted to any university. All sources have been referred to and give adequate credit to others for their work, and I, in no way, claim to have created this information myself.

Location and Date	Signature

Table of Contents

List of Figures

List of Tables

List of Acronyms

CFmask	C Function of mask
EO	Earth observation
ETM+	Enhanced Thematic Mapper Plus
FAO	Food and Agriculture Organization of the United Nations
Fmask	Function of mask
GEE	Google Earth Engine
GIS	Geographic Information System
GSW	Global Surface Water
IFOV	Instantaneous Field Of View
JRC	Joint Research Centre
LaSRC	Landsat Surface Reflectance Code
LEDAPS	Landsat Ecosystem Disturbance Adaptive Processing System
LULC	Land use and land cover
MRD	Mekong River Delta
NDWI	Normalised Difference Water Index
NIR	Near-infrared
OLI	Operational Land Imager
PRD	Pearl River Delta
RRD	Red River Delta
RS	Remote sensing
SAR	Synthetic Aperture Radar
SR	Surface Reflectance
TM	Thematic Mapper
ToA	Top of Atmosphere
USGS	U.S. Geological Survey
YRD	Yellow River Delta

1 Motivation and Background

1.1 Anthropogenic LULC Change

Ever since humans stopped to migrate and settled down to farm within seven or eight regions throughout the world (Bellwood, 2007), they began to reorganise natural conditions and to create their individual structures, which constantly remained for longer periods. The Neolithic Revolution has begun and has enabled an increasingly larger population (Bocquet-Appel, 2011). With a growing world population, alterations took place at an accelerated rate and many parts of the earth's surface have been exposed to heavy Land use and land cover (LULC) change until the present day: deforestation, agriculture, mining, urbanisation. All of these alterations determine a variety of factors, such as the radiation balance (Cui et al., 2012), carbon cycle (Arneth et al., 2017), water balance, ecosystem functioning, biodiversity (Falcucci et al., 2007) and links among these. A major part of LULC changes took place in the tropics (Gibbs et al., 2010), which are meaningful for nature conservation, as these often coincide with biodiversity hotspots (Myers et al., 2000). LULC changes and the often accompanied decrease of natural habitats, as well as global climate change are assumed to be the most threatening factors for biodiversity at present and in the future (Sala et al., 2000; Jetz et al., 2017). Species currently at risk by changing climate are exposed to additional pressure caused by LULC change. For this century, even more dramatic consequences evoked by environmental change are expected (Sala et al., 2000). Understanding and monitoring these complex interactions is the first step to counteract ecosystem harming and to define management strategies (Alexandridis et al., 2008).

1.2 Earth Observation as a Powerful Tool to Reveal LULC Change

Satellite remote sensing (RS) and geographic information system (GIS) techniques are powerful tools to map and monitor the extent and patterns of LULC changes on large spatial scales. They are cost- and time-efficient and with increasing access to satellite imagery due to growing free data policy (Woodcock et al., 2008; Wulder et al., 2012), they are also greatly appreciated by ecologists and nature conservationists. This can also be seen in the rising number of publications related to RS topics and their applications within this field (Seto and Fragkias, 2007; Turner et al., 2015; Pettorelli et al., 2017; Young et al., 2017). If suitable satellite imagery is available for the desired time period, investigations can be undertaken retrospectively. This is especially helpful in evaluating long-term changes, for which constant and long-term

observational data are essential. Assessing and monitoring malfunctions of ecosystems caused by human pressure is crucial to achieve attention and emphasise the need for policy to act (Alexandridis et al., 2008).

1.3 Aquaculture as an Intensive LULC Change

One major LULC change of the last decades in coastal areas can be attributed to the expansion of aquaculture. Aquaculture defines any sort of aquatic organisms farmed and harvested in aquafarms which are almost exclusively destined for human food consumption (FAO, 2016). In general, two types of aquaculture can be differentiated, which is inland aquaculture (freshwater, brackishwater or saline water) and marine aquaculture (Cosslett and Cosslett, 2014). The majority of aquaculture is farmed in inland aquaculture basins, accounting for 63 % of global production (FAO, 2016). Aquaculture farming requires the use of inputs of natural resources, such as land, water and aquatic species, as well as non-natural resources, such as feeds, antibiotics and artificial fertilisers (FAO, 2016). Aquaculture farming can be operated on different levels of professionalism, which comprise highly industrialised aquafarms but also small-scale household subsistence farming. In some regions, it is a common practice to carry on a mixed form of aquaculture and rice cultivation (Ottinger et al., 2016). Various forms of fish, molluscs, crustaceans and plants can be grown, which can be produced according to local conditions, as they tolerate different amounts of salinity (Cosslett and Cosslett, 2014).

Asia is the hotspot region of global aquaculture production, accounting for 88.9 % in 2014, followed by North and South America with 4.5 %, Europe with 4.0 %, Africa with 2.3 % and Oceania with 0.3 % (FAO, 2016). Thirteen Asian nations are among the top 25 producers of farmed aquatic species (Figure 1.1). The increase in aquaculture production for China and Vietnam has been enormous between 1995–2014 (Figure 1.2). Country-wise, China is by far the top producer which contributed 61.6 % to the aquaculture production worldwide in 2014. The Vietnamese aquaculture production accounted for 5.77 % of the global production and is ranked on fourth place of top producing countries (FAO, 2016).

The enormous quantities of aquaculture goods produced in Asian aquafarms require high amounts of land. Therefore, aquaculture is one of the major drivers of LULC change within coastal regions, at the expense of floodplains and wetlands (Alonso-Pérez et al., 2003; Ke et al., 2011; Pattanaik and Narendra Prasad, 2011), also including the deforestation of mangrove forests (Valiela et al., 2001). Coastal areas are hotspots of species richness and biodiversity (Diana, 2009) and, therefore, focus regions for conservational efforts. Despite the heavy pressure on valuable natural land cover, the Vietnamese convention on preserving wetlands did not show success on reducing the expansion of aquaculture but wetland retreat increased (Seto and Fragkias, 2007). Similar findings of decreasing natural coastal land cover and, simultaneously, expansion of aquaculture area have been stated in numerous case studies (Béland et al., 2006; Berlanga-Robles et al., 2011; Pattanaik and Narendra Prasad, 2011; Richards and Friess, 2016)

The Food and Agriculture Organization (FAO) provides information and statistics on fisheries and aquaculture in regular intervals to increase transparency and to optimise the system of aquaculture to preserve food security and to contribute to human well-being (FAO, 2016). However, data acquisition is arduous as the sub-

mitted national statistics are not based on standardised methods. The reliability of the provided data is questionable and improved monitoring is demanded (Pauly and Zeller, 2016). Therefore, RS serves to provide additional and objective information of aquaculture development and its provoked LULC changes.

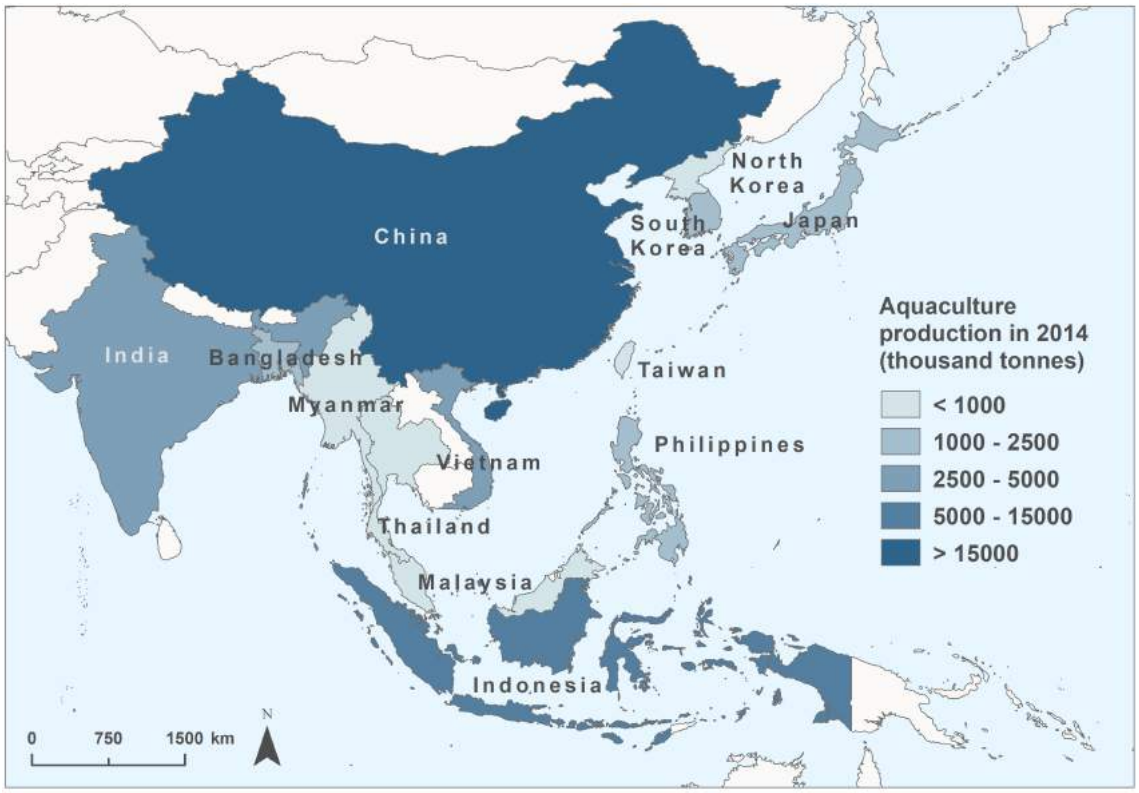

Figure 1.1: Asian countries which are among the top 25 producers of aquaculture worldwide. Data retrieved from: FAO (2016).

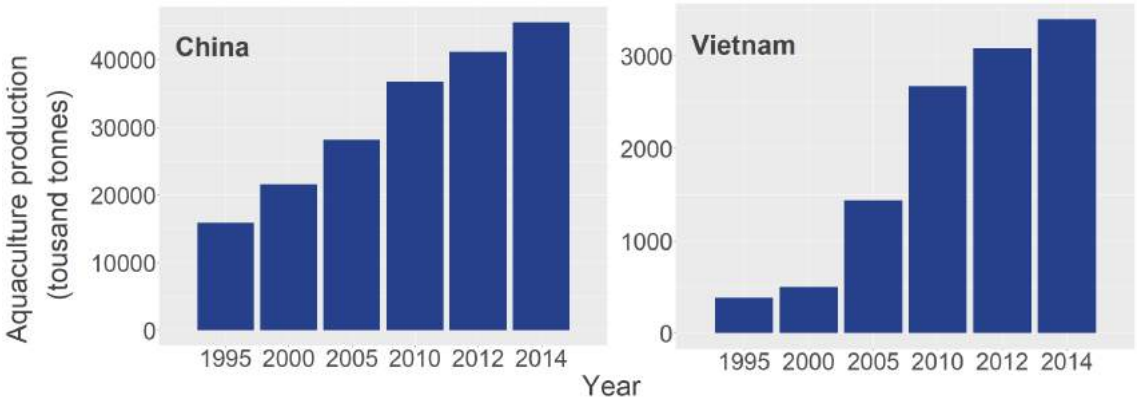

Figure 1.2: Aquaculture production in China and Vietnam. Data retrieved from: FAO (2016).

2 Analysing Spatio-temporal Patterns of Coastal Aquaculture Based on Three Decades of Satellite Data

Abstract

Asia is the major contributor to global aquaculture production in quantity, accounting for almost 90 % of farmed species. These practices lead to extensive land use and land cover changes in coastal areas, and thus harm valuable and sensitive coastal ecosystems. RS and GIS technologies contribute to the mapping and monitoring of changes in aquaculture providing essential information for coastal management applications. This study aims to investigate aquaculture expansion and spatio-temporal dynamics in four Asian river deltas over three decades: the Yellow River Delta (YRD), the Pearl River Delta (PRD), the Red River Delta (RRD) and the Mekong River Delta (MRD). Long-term patterns of aquaculture change are derived based on combining existing aquaculture information for recent years with information extracted from the Landsat long-term archive. Furthermore, the suitability of the proposed approach to be applied on a global scale is tested based on exploiting the Joint Research Centre (JRC) Global Surface Water (GSW) dataset. Enormous increases in aquaculture area were detected for all investigated target deltas: an 18.6-fold increase for the YRD (1984–2016), a 4.1-fold increase for the PRD (1990–2016), a 1.6-fold increase for the RRD (1990–2016) and a 7.2-fold increase for the MRD (1989–2015). Furthermore, hotspots of aquaculture expansion were detected based on linear regression analyses for the Chinese target deltas, indicating that hotspots are located in coastal regions for the YRD and along the Pearl River in the PRD. A comparison with high resolution Google Earth Data demonstrates that the proposed approach is able to detect spatio-temporal changes of aquaculture at an overall accuracy of 71 %. The presented approach has the potential to be applied on larger spatial scales covering a time period of more than three decades. This is crucial to define appropriate management strategies in order to reduce the environmental impacts of aquaculture expansion which are expected to further increase.

Keywords: aquaculture; Landsat; earth observation; remote sensing; temporal analysis; river delta; coastal region; Asia;

2.1 Introduction

Aquaculture has experienced a remarkable global production increase in the last decades which has more than tripled from 1995–2014 to approximately 74 million tonnes (FAO, 2016). This trend is evoked by a variety of factors. Among others, continuing growth of world population, globalisation and high market values of traded aquaculture commodities can be named (Ottinger et al., 2016). In this regard, aquaculture has been promoted as a big contributer to global food security, as an alternative to capture fisheries and entails an economic upswing for developing and threshold countries. However, concerns about the environmental impact of aquaculture farming have been rising, especially on the evidence that aquaculture will surpass fishery production, which has already happened in the Asian region (FAO, 2016). Therefore, aquaculture production and its implications for society and the environment have become a hot topic in science and policy.

Aquaculture, as a high-value export good, opens up new market opportunities for developing countries. Aquaculture is the sector of food production systems with highest growth rates. For the Vietnamese economy, the MRD as a top producing region for aquaculture plays an important role, thereby has a higher gross domestic product growth than the rest of the country (Cosslett and Cosslett, 2014). Several studies pointed out that aquaculture has the potential to reduce poverty across the world (Irz et al., 2007; Kaliba et al., 2007; Pant et al., 2014). Due to population growth, aquaculture as a controlled system of protein production is powerful in contributing to food security and to cover future nutrition demands, which positively influences human well-being (Herbeck et al., 2013). In addition, growing seaweed proofed to remove nutrients to counteract eutrophication of water bodies (Xiao et al., 2017).

However, the negative effects of aquaculture production on the state of the environment, especially the animal producing sector, is evident. The aquaculture industry is heavily polluting the surrounding waters both freshwater bodies or streams and sea water. Wastewater created during aquaculture production is often discharged unfiltered, causing accumulation of pharmaceuticals (He et al., 2016) and heavy metals (Liang et al., 2016), accelerating eutrophication (Herbeck et al., 2013) and enhancing harmful algal blooms (Wang et al., 2008; Keesing et al., 2011; Lee et al., 2011). To make room for aquaculture ponds in coastal areas, mangrove forests get logged, which contribute to coastal protection, are key nursery habitats and were found to positively impact filtration, e.g. of heavy metals (Nguyen et al., 2015; Nguyen van et al., 2016). Heavy metals originating in industry can already be detected in aquaculture products (Cheng et al., 2013) and the amounts even exceed Chinese safety guidelines (Liang et al., 2016). Besides pollution and deforestation of mangroves, the water consumption of aquaculture production leads to excessive extraction of ground water which increases salinity (Ha et al., 2018). Through groundwater pumping in the YRD, subsidence rates are higher than local and global sea level rise, which exposes Asian megadeltas to various dangers like storm surges, salinate groundwater, intensified flooding and shoreline retreat (Higgins et al., 2013). In addition, the positive effect of aquaculture on sustaining fish stocks (Stotz, 2000) has to be doubted, as most of the aquafeeds are made from fishmeal and fish oil (Hardy, 2010), which is produced from wild catch and consequently puts additional pressure on fish stock (Naylor et al., 2000; Pauly and Zeller, 2017).

Despite the fact, that aquaculture production is detrimental to the environment, it will further expand (Pauly and Zeller, 2017). In this context, it is fundamental to assess the dimensions of aquaculture and provide solid data for management applications. The FAO provides the only global database on fisheries and aquaculture which is commonly used in science and policy (Garibaldi, 2012). However, the reliability of this database has been called into question, assuming that numbers are underestimating reality (Pauly and Zeller, 2016, 2017). RS technologies can serve as an useful tool to determine aquaculture extent and its dynamics and results may operate as an additional and independent source of data. Additionally, spatio-temporal patterns of aquaculture become discernible which is crucial for the management of its expansion and its resources, to guarantee for the maintenance of its positive implications and to lower its negative effects.

Different approaches exist to observe and quantify aquaculture based on RS and GIS techniques using Landsat imagery. To assess bitemporal changes in shrimp aquaculture, supervised classification approaches have been applied (Alonso-Pérez et al., 2003) and change detection methods were undertaken to reveal the influence of aquaculture on coastal ecosystems (Béland et al., 2006; Rajitha et al., 2010; Berlanga-Robles et al., 2011; Bui et al., 2014; Peneva-Reed, 2014). However, the majority of these studies investigate small-scale regions, e.g. single bays or lagoons (Alonso-Pérez et al., 2003; Bui et al., 2014), a few villages (Peneva-Reed, 2014) or parts along the coastline (Béland et al., 2006; Berlanga-Robles et al., 2011) and rather focus on the quantification of aquaculture area. To identify trends of aquaculture, time series assessments on large scales are needed. Therefore, Landsat data provides the ideal basis to firstly, carry out an assessment on large spatial to global scales and, secondly, to detect spatio-temporal patterns of aquaculture expansion on multitemporal scales. However, the spatial resolution of Landsat imagery is not sufficient to accurately map aquaculture on single pond level, which is crucial to assess spatio-temporal dynamics within the deltas. Thus, high resolution data is necessary to accurately map aquaculture ponds and quantify their size and shape, especially to distinguish between single aquaculture ponds (Ottinger et al., 2017).

Therefore, to cover the spatial requirements for this analysis, aquaculture pond layers based on Sentinel-1 imagery serve as the basis of this study, which are kindly provided by Ottinger et al. (2017). To cover the temporal components of this assessment, Landsat Surface Reflectance (SR) data are used, thereby exploiting the large potential of the open Landsat archive with multispectral satellite data spanning time periods of more than 30 years. With the focus on Asian coastal aquafarms, the goal of this study is to estimate increases in aquaculture area and to reveal the dynamics and possible hotspots of aquaculture expansion in coastal areas of four target deltas in China and Vietnam. It is assumed that aquaculture area has increased over the observed time period for all four study sites. In addition, it is hypothesised that hotspots of aquaculture can mainly be detected close to water sources, such as coastal areas and along the river course. Furthermore, the results of this study serve to demonstrate potentials and limitations of aquaculture quantification through long-term Landsat imagery and to highlight differences in the assessment among the case study regions. The results are compared with assessments based on GSW data which potentially serves to apply the approach on larger scales.

2.2 Study Area

The study area comprises four river deltas: the YRD and the PRD in China and the RRD and the MRD in Vietnam (Figure 2.1).

The YRD is the smallest out of the four investigated deltas and shows the smallest population (Table 2.1). The delta is located at the Chinese east coast in the province Shandong. The Yellow River has a comparatively low water flow but transports the highest sediment loads worldwide which originate in the country's Loess Plateau and supply the floodplains with valuable nutrients (Ren, 2015). It has also great power of erosion, is shifting its course and delta mouth continuously and has been responsible for numerous dike breaches and floods (Higgins et al., 2013; Ren, 2015). The delta region suffers from rapid economic growth and urban expansion, both accompanied with heavy pollution, as can be seen for many parts of Chinese coastlines (Li et al., 2009; Ottinger et al., 2013; Wohlfart et al., 2016; Li et al., 2017). In addition, groundwater extraction reaches alarming proportions, mainly caused by aquaculture, and the salt content exceeds that of seawater in some parts of the delta (Higgins et al., 2013).

Among the study regions, the PRD is the biggest and most populated delta (Table 2.1) and lies within the center of the Guangdong province. The delta includes mega-cities with a population of more than 10 million like Guangzhou and Shenzhen as well as other multi-million cities. The whole delta is undergoing enormous urbanisation processes and single cities tend to become one large interwoven urban complex (Zhao et al., 2017). Before the economic boom took place, the delta played an essential role for Chinese agriculture, but big parts of the land have been transformed to building land (Li and Yeh, 2004). Nonetheless, the majority of population is still living in non-urban parts and agriculture is a popular practice within the PRD. Heavy metal pollution originating from industry and aquaculture is a big concern within this area which is also evident within farmed aquatic species destined for food consumption (Liang et al., 2016). The use of pharmaceuticals in aquaculture is further accelerating pollution processes (He et al., 2016). Many coastal areas in China have to deal with heavy pollution, but the PRD exceeds the usual parameters (Liang et al., 2016).

The RRD and the MRD belong to the top producing regions of agricultural commodities in Vietnam. In 1986 the doi moi (renovation) reformers were initiated by the government to increase productivity and attraction for foreign investors (Seto and Fragkias, 2007). This radical change has led to major LULC changes within the whole country, promoting intensified agriculture with high yields of valuable goods (Seto and Fragkias, 2007). Within the RRD in northern Vietnam, the capital Hanoi is located at the course of the Red River (Figure 2.1). The delta is densely populated and has a total population of approximately 20.2 million (Table 2.1). The region's climate is determined by a rainy season between May and October, followed by a dry season from November to April (Nguyen et al., 2015). The increase in aquaculture farming can be seen in numbers on aquaculture production from approximately 55,600 tonnes in 1995 to 580,915 tonnes in 2015, which is a ten fold increase within 10 years (General Statistic Office of Vietnam, 2015).

The MRD is the most southern part of Vietnam and borders on Cambodia in the northwest (Figure 2.1). The climate is tropical monsoonal with a dry season from December to May, but humidity remains high throughout the year (Cosslett

and Cosslett, 2014). As a consequence of permanent water supply through the Mekong and the tidal influence from the South China Sea (Cosslett and Cosslett, 2014), the delta is of great importance for the agricultural sector. The region is accompanied with high production of paddy rice and aquaculture and, therefore, essential for Vietnam's economy. About 2.6 million ha are used for agriculture, for which rice production itself accounts for 2 million ha (Ha et al., 2018) and requires 65 % of the available freshwater (Cosslett and Cosslett, 2014). Aquaculture has rapidly developed to a top export commodity and is pushing away from subsistence farming towards a more profit-oriented agriculture operated by companies (Cosslett and Cosslett, 2014). Another reason for the rise in aquaculture production is the increasing salinity in the southern coastal areas. Farmers are shifting from rice cultivation to saline, brack-water shrimp farming (Cosslett and Cosslett, 2014). Along the delta's coastline, mangrove forests are getting re-established after being excessively logged during the 1980s and 1990s, mainly due to aquaculture and shrimp farming (Cosslett and Cosslett, 2014).

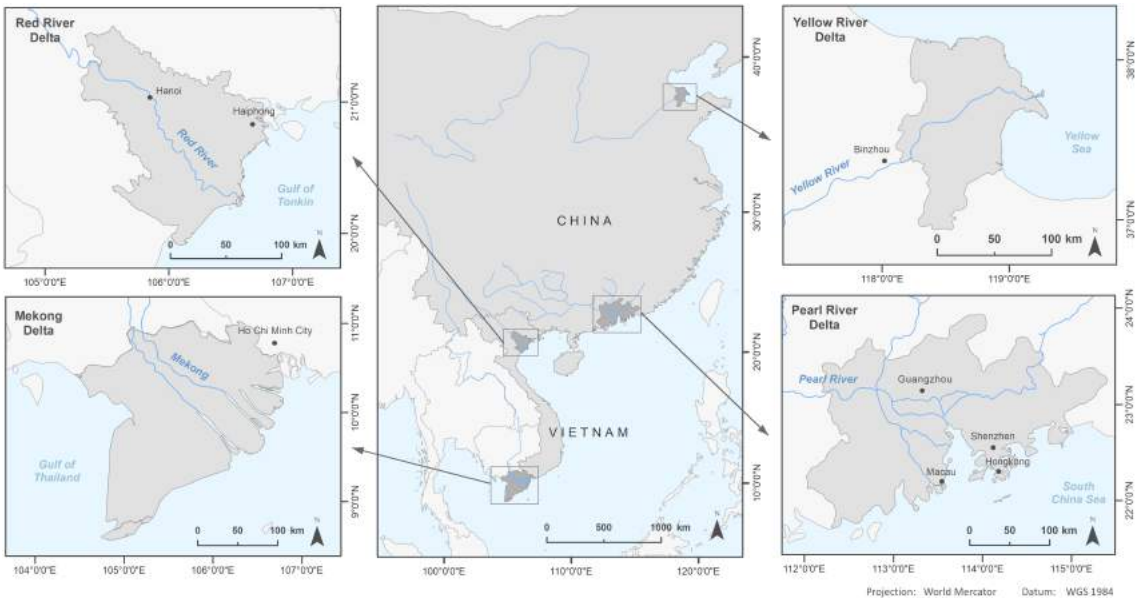

Figure 2.1: Map of the four investigated deltas.

Table 2.1: Characteristics of the investigated deltas (adapted from Ottinger et al. 2017).

		Delta size (km^2)	Delta population (millon)	Delta coastline (km)
China	Yellow River Delta	7,500	5.9	389
	Pearl River Delta	42,300	57	1,857
Vietnam	Red River Delta	15,500	20.2	187
	Mekong Delta	39,300	18	999

2.3 Materials and Methods

2.3.1 Data

2.3.1.1 Landsat Surface Reflectance Data

In this study, multispectral Level-2 Landsat SR data are used. The Landsat program builds an ideal basis to answer the above stated research questions, as it provides a continuous time series of satellite data, starting in 1972 with Landsat 1 and continuing until now with its latest satellite Landsat 8 and with imagery free of charge. Although Landsat 1, 2 and 3 were operating from 1972 onwards, only data from Landsat 4 (1982–1993) and Landsat 5 Thematic Mapper (TM) (1982–2012), Landsat 7 Enhanced Thematic Mapper Plus (ETM+)(1999–2017) and Landsat 8 Operational Land Imager (OLI)(2013–2017) are taken into consideration, as they provide an identical spatial resolution of 30 m. Downsampling methods are not applied, as they are rather work intensive and need accurate geo-referencing (Almonacid-Caballer et al., 2017). In addition, the envisioned data is covering a potential time period from 1982 until now and most of the remarkable alterations in aquaculture farming have been taken place in recent decades (FAO, 2016).

The Level-2 SR data guarantee for atmospheric correction following the principles of the Landsat Ecosystem Disturbance Adaptive Processing System (LEDAPS) for Landsat 5 and 7 imagery (Masek et al., 2006) and the Landsat Surface Reflectance Code (LaSRC) for Landsat 8 imagery (U.S. Geological Survey). In addition, the SR data contain the so-called CFmask band. The band provides values 0–4 for five classes, where 0=clear, 1=water, 2=shadow, 3=snow and 4=cloud. Therefore, it can be used for masking disturbing pixels containing clouds or cloud shadows within Earth Observation (EO) data and was found to perform best among other cloud masking algorithms (Foga et al., 2017). It is based on the Function of mask (Fmask) algorithm, initially created in MATLAB (Zhu and Woodcock, 2012) and was later transferred to the C language to enhance it's efficiency (Foga et al., 2017). The Landsat SR data are originally provided by the U.S. Geological Survey (USGS) but are assessed and processed through the Google Earth Engine (GEE) platform. The GEE is a cloud-based platform, providing a multi-petabyte ready to use data catalogue and the respective computational resources for quick and effective online processing (Gorelick et al., 2017).

In total 5,213 Landsat SR scenes were processed in this study, of which 76 % originate from Landsat 5, followed by 7 % and 17 % originating from Landsat 7 and Landsat 8, respectively. For the YRD a total of 1,908 scenes are used which are sufficient to generate cloud free image composites for every year between 1984 and 2016 (Figure 2.2). For the PRD a total of 2,124 scenes are used with no information for the years 2010, 2012, and 2015 due to insufficient data coverage. For the RRD, heavy cloud cover results in major data gaps throughout the entire observation period, which reduces annual data coverage below the feasible limit for assessing yearly aquaculture dynamics. Therefore, multi-annual composites are produced for the time periods 1990–1994, 1995–1999, 2000–2004, 2005–2009 and 2013–2016. The period 2010–2012 is excluded due to insufficient data coverage and high cloud cover. For the MRD, Landsat SR data are only available for a limited number of years making it impossible to use the Landsat SR data in the proposed

approach. Therefore the JRC GSW data set (Section 2.3.1.3) was used instead to analyse the aquaculture dynamics for this study region.

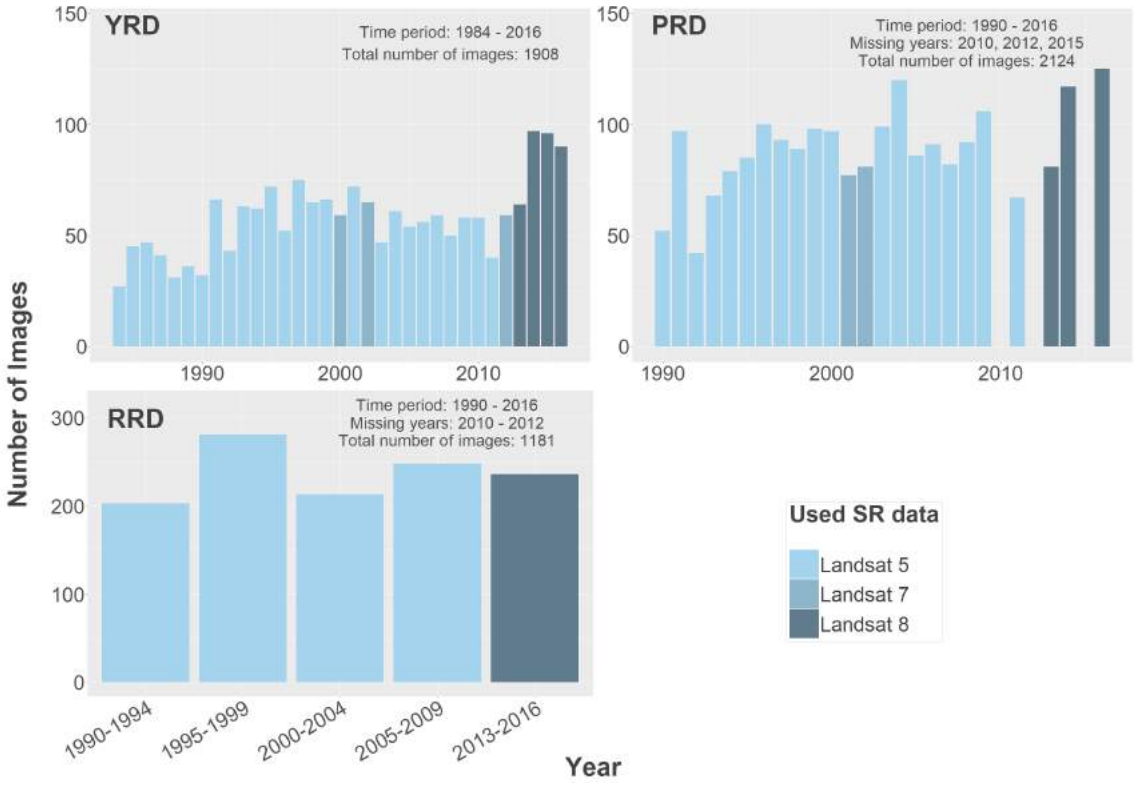

Figure 2.2: Used Landsat SR data for creating the annual water masks for the YRD, the PRD and the RRD. The bar colours indicate the used Landsat SR data. For the MRD, Landsat SR data were insufficient and, hence, the JRC GSW data set was used instead for this study region.

2.3.1.2 Sentinel-1 Aquaculture Layer

Although the Landsat program provides data for a long time period, Landsat's spatial resolution of 30 m is a limiting factor for detecting small scale features such as aquaculture ponds (Ottinger et al., 2017; Phiri and Morgenroth, 2017). Especially aquaculture farming on household scale is characterised by rather small water ponds (Ottinger et al., 2017) below 900 m^2 corresponding to the Instantaneous Field of View (IFOV) of the Landsat sensors. Furthermore, due to the narrow dams between individual aquaculture ponds, water areas are often recognised, but will not show accurate detection of single aquaculture ponds and would probably fail to guarantee for assessing the diverse structures of aquaculture. Therefore, this study combines the advantage of high spatial resolution Sentinel-1 data for precise aquaculture pond mapping with the temporal component of Landsat imagery for analysing historical patterns and dynamics of aquaculture.

Therefore, for each delta an aquaculture mask, derived from Sentinel-1 time series data, is used in this thesis to reflect the actual aquaculture structures at pond level. These layers in vector format (Figure 2.4) were kindly provided by Ottinger et al. (2017) and are termed as Sentinel-1 Layers in further explanations. The authors used 10 m resolution Sentinel-1A Synthetic Aperture Radar (SAR) data acquired between September 2014 and September 2016 in an object-based classification approach to

extract aquaculture ponds, resulting in an overall accuracy of 0.83 for all four river deltas. The definition of aquaculture is based on several criteria like the geometry of aquaculture ponds (area and perimeter), two compactness metrics, the slope of location and the exclusion of standing water areas. For detailed information on the approach and results consult the study of Ottinger et al. (2017).

Table 2.2 shows some general characteristics of the aquaculture ponds derived from the Sentinel-1 Layers for the four target regions. It can be seen that the mean aquaculture pond size is by far biggest for the YRD (43,450.2 m^2), followed by the MRD (8873.6 m^2), RRD (4885.1 m^2) and PRD (3966.5 m^2). Considering the distribution of aquaculture pond size among the deltas, nearly all ponds in the YRD are larger than 900 m^2 with 1.2 % and, therefore, the chance of being detected on the basis of 30 m Landsat imagery is high. In the remaining deltas, small ponds below 900 m^2 make up large proportions –up to more than one third of all ponds– and, therefore, an approach based on Landsat data alone can be expected to have less precise results.

Table 2.2: Characteristics of the aquaculture ponds retrieved from the Sentinel-1 Aquaculture Layers.

	Yellow River Delta	Pearl River Delta	Red River Delta	Mekong River Delta
Number of ponds	19070	264894	61289	299649
Mean pond size (m^2)	43450.2	3966.5	4885.1	8873.6
Pond size < 900 m^2 (%)	1.2	16.8	23.1	38.9
900 ≤ pond size ≤ 1,800 m^2 (%)	15.8	27.8	29.2	17.7
1,800 ≤ pond size ≤ 5,000 m^2 (%)	31.2	36.8	29.0	21.6
5,000 ≤ pond size ≤ 10,000 m^2 (%)	14.6	11.9	9.6	9.4
10,000 ≤ pond size ≤ 50,000 m^2 (%)	25.9	6.2	7.8	9.6
50,000 ≤ pond size ≤ 100,000 m^2 (%)	4.6	0.3	0.8	1.3
Pond size > 100,000 m^2 (%)	6.7	0.2	0.4	1.4

2.3.1.3 The Global Surface Water Data

A global raster data set on inland water surfaces, the so called GSW data set is used in this study as an alternative to custom tailored water masks derived from the Landsat SR data archive. This has two reasons: first, the GSW data set is used as the main data source for the analysis in the MRD for which Landsat SR data are not available. Second, the GSW data set is used in a comparative analysis in the remaining three deltas to asses its use as an readily available substitute data source for a potential global scale application. In addition, the GSW data set is used to asses natural water bodies for the first year of observation that have been turned to aquaculture ponds in subsequent years, in the course of the accuracy assessment (Section 2.3.4). The GSW dataset by Pekel et al. (2016) consists of a variety of products containing data on global water dynamics and extents. It can be assessed through the GSW Explorer initiated by the European Commission's JRC (European Commission, 2016). For this study, the yearly history dataset is used, which is available via the GEE platform. The data contain four classes: 0=no data, 1=not water, 2=seasonal water and 3=permanent water. It is based on Landsat Top of Atmosphere (ToA) data and is available until the year 2015.

Annual data were consistently available from 1984–2015 for the YRD. However, data coverage was not sufficient for the other deltas and several years had to be excluded for further analysis. The analysis was undertaken from 1988–2015 for the

PRD, but data was missing for 1989, 1992–1995 and 1997-1999. The aquaculture of the RRD was again observed for 5-year intervals from 1990–2009 and a 3-year interval for 2013–2015. For the MRD, for which only insufficient Landsat SR data are available, patterns are analysed for 1989–2015 with missing data for the years 1987, 1988 and 1990–1998.

2.3.2 Assessment of Aquaculture Dynamics

Spatio-temporal aquaculture dynamics are assessed by combining current aquaculture structures at pond level derived from Sentinel-1 data with annual water masks derived from historic Landsat data. Thereby this methodological approach is based on the simplified assumption that 1) due to the continuous and rapid development of aquaculture worldwide, current pond structures resemble the maximum status of aquaculture expansion compared to previous years and 2) that identified ponds for the reference year 2016 are also highly likely to be ponds in a previous year when permanently filled with water during this specific year.

The annual water masks for each delta region are generated according to the following six steps (Figure 2.3): firstly, for every target year all available Landsat images are selected and cloud and cloud shadow masking is performed based on the CFmask band. Secondly, the Normalised Difference Water Index (NDWI) is calculated for every Landsat image to better identify surface waters within the deltas. The NDWI formula after McFeeters (1996) using the GREEN and NIR band is applied, as it is the most common in detecting open water bodies in the field of applications in EO. The index is defined as

$$NDWI = \frac{GREEN - NIR}{GREEN + NIR}. \tag{2.1}$$

The third step focuses on the exploitation of the temporal characteristics of aquaculture ponds. Aquaculture ponds can be generally described as permanent water bodies, in contrast to e.g. temporarily inundated rice paddy fields, which are the main source of confusion in this approach. Therefore temporal metrics, i.e. the 10th and the 90th percentiles are calculated based on all cloud free NDWI observations for each pixel. The difference of the the lowest (10th percentile) and highest (90th percentile) NDWI values within the year, serves as a good indicator for the persistence of inundation supporting the accurate differentiation between aquaculture and rice paddy fields. Fourth, a threshold was set to separate pixels attributed to land or water, which results in a binary permanent water-land mask for each delta. The threshold for every river delta was defined empirically by trial and error and was validated by interpreting high resolution Google Earth imagery.

In the fifth step, the binary land-water mask derived from Landsat was combined with the Sentinel-1 Aquaculture layer and the proportion of water area within each pond was computed. In the last step only those ponds were selected as correctly identified aquaculture ponds that showed a certain minimum percentage of water coverage. Thereby different thresholds were empirically tested and finally set to 33 %. The rather low percentage can be explained by the different data sources (SAR versus multispectral) and spatial resolutions (30 m versus 10 m) as can be seen in Figure 2.4. It is evident that detected water surfaces and pond structures show generally corresponding patterns, however, do not match perfectly to each other.

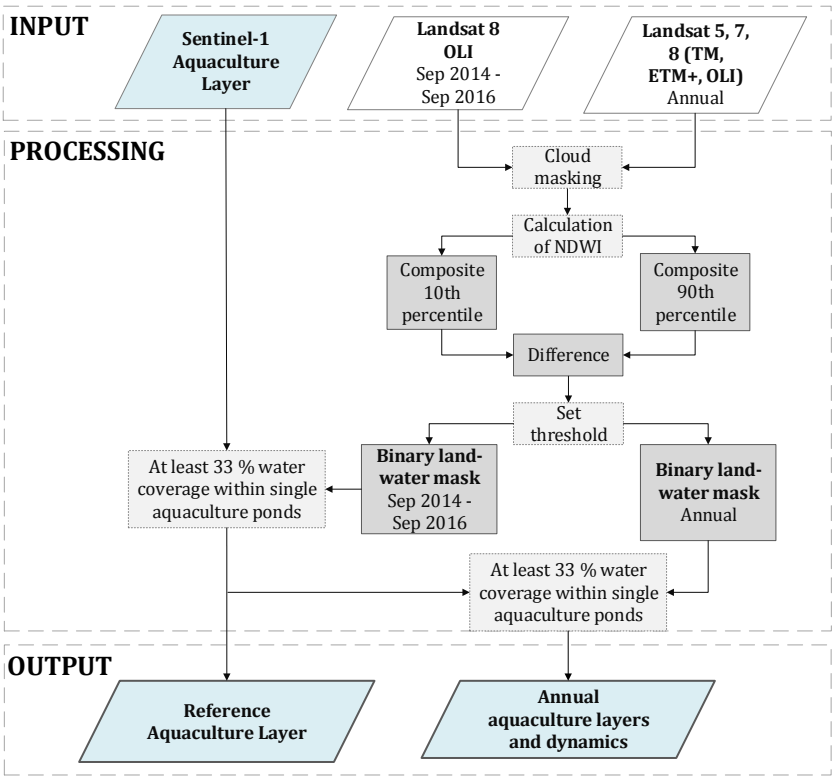

Figure 2.3: Workflow diagram on creating the Reference Aquaculture Layer and assessing aquaculture dynamics.

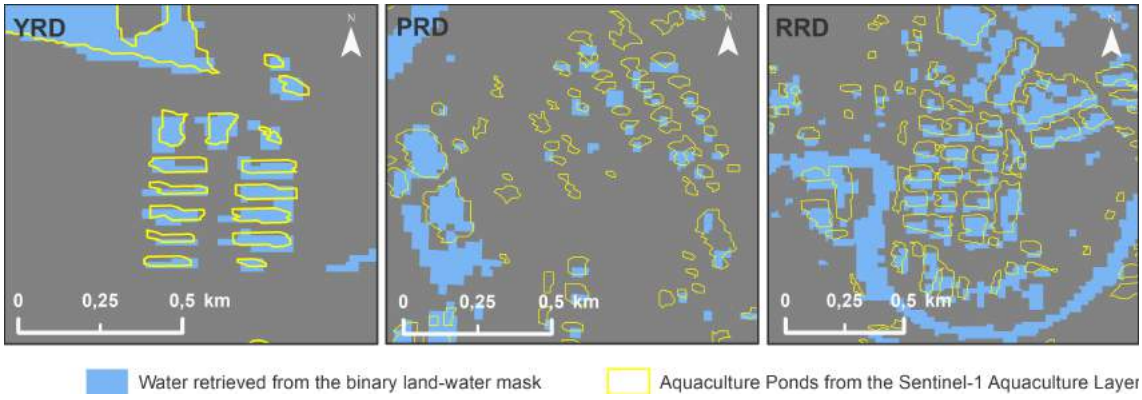

Figure 2.4: The challenges on combining the Sentinel-1 Aquaculture Layer with Landsat satellite data evoked by different spatial resolution. One exemplary detail map for each investigated delta is shown (from left to right: YRD, PRD and RRD). The different spatial resolution of the input data requires an appropriate approach to combine both datasets, as water detection based on Landsat data is very different from the aquaculture structure retrieved from the Sentinel-1 Aquaculture Layer.

For the YRD and PRD this approach is followed for every year where Landsat data are available while for the RRD multiannual time steps are applied, as described in Section 2.3.1.1. For the MRD no adequate Landsat data were available. For the YRD, PRD, and RRD, the latest aquaculture layer incorporates all Landsat data between September 2014 and September 2016. This so called Reference Aquaculture Layer corresponds to the observation period of the Sentinel-1 Aquaculture layer and

serves as baseline for all previous years. Furthermore, for all four deltas additional aquaculture layers were generated on the basis of the GSW data set for all years for which respective GSW data were available. This was done by replacing step 1–4 with the annual water masks from the JRC GSW dataset.

2.3.3 Temporal Patterns and Hotspots

To retrieve hotspots of aquaculture expansion and to detect their temporal patterns within the target deltas, a linear regression analysis was carried out. For this purpose, the deltas assessed with Landsat SR data (YRD, PRD and RRD) were divided into a hexagon landscape. The hexagon diameters are chosen to be the same for each delta with 4000 m at their greatest spacing, to easily enable comparisons among the deltas. The aquaculture polygons are converted into point data and are distinctly assigned to the hexagon which they fall into. The point data includes information on the aquaculture pond area and the area is summed up for each hexagon and each year. To reveal aquaculture patterns and development over time, a linear regression analysis was conducted, thereby, time is the explanatory variable and the aquaculture area is the response variable. The regression analysis was undertaken for each hexagon of the delta landscape, which resulted in a total of 4,349 individual regression analyses (494 for the YRD, 2,852 for the PRD and 1,003 for the RRD).

2.3.4 Accuracy Assessment

The aim of the accuracy assessment in this study is to evaluate whether aquaculture dynamics are correctly detected through the proposed approach. The PRD serves exemplary for validating the approach on assessing the temporal dynamics within the delta regions since this delta showed the best coverage of high resolution satellite data for different time points throughout the observation period. Reference data were collected using high resolution imagery available via Google Earth, which is a frequently used source for ground truth reference data in RS studies (Khorram et al., 2012). In order to include as many time points as possible in the assessment all high resolution data available for the PRD were evaluated within the observation period covering the years 2004, 2005, 2006, 2008, 2011, 2014, and 2016. To compare the agreement of prediction data and reference data, two classes were created: 1) aquaculture ponds in the Reference Aquaculture Layer that were also detected as aquaculture in the year of evaluation (class: stable aquaculture) and 2) aquaculture ponds in the Reference Aquaculture Layer that have not been detected as aquaculture in the year of evaluation (class: aquaculture change). In total, 200 aquaculture ponds were chosen by stratified random sampling for each of the two classes and evenly over all years of evaluation.

The results on the accuracy assessment are shown in a confusion matrix and the standard measures of accuracy, i.e. the producer's, the user's and the overall accuracy as well as Cohen's Kappa (Cohen, 1960) were calculated. The value of the Kappa index is associated with different levels of agreement: <0 = no agreement, 0–0.20 = slight agreement, 0.21–0.40 = fair agreement, 0.41–0.60 = moderate agreement, 0.61–0.80 = substantial agreement, and 0.81–1 = almost perfect agreement (Landis and Koch, 1977).

With respect to the assumptions stated in Section 2.3.2 permanent natural water

bodies that are converted to aquaculture in later years are one source of error leading to overestimations of aquaculture. These water areas are generally identified as aquaculture throughout the entire observation period regardless of their actual time point of conversion. Therefore, based on the GSW data, annual water masks of the starting year of investigation for each delta assessed with Landsat SR data (YRD, PRD and RRD) are retrieved. Artificial water surfaces like aquaculture ponds are removed manually by visual interpretation with the help of high resolution Google Earth imagery. This results in a layer with natural water bodies for each delta and year, in which the observation period started: 1984 for the YRD, 1990 for the PRD and 1990–1994 for the RRD. For the latter, the yearly GSW data from 1990–1994 were mosaicked before creating the water mask. On the basis of these layers, for each delta those natural water bodies are identified that have been converted to aquaculture in later years during the observation period. The proportion of these erroneously identified ponds (false positives) in relation to all ponds can be used as indicator for the degree of uncertainty related to this error.

2.4 Results

2.4.1 Reference Aquaculture Layer

A comparison of detected ponds and pond area for the Sentinel-1 Aquaculture Layer and the Reference Aquaculture Layer for all three deltas is shown in Table 2.3. In the YRD, around 80 % of ponds in the Sentinel-1 Aquaculture Layer were sufficiently covered with water as observed from the Landsat water mask and, therefore, were also defined as aquaculture in the Reference Aquaculture Layer. This high proportion of detected ponds for the YRD is followed by around 63 % for the PRD and roughly 50 % for the RRD. When considering the detected aquaculture area, numbers increase to 95 % for the YRD, 81 % for the PRD and 79 % for the RRD.

Table 2.3: Comparison of Sentinel-1 Aquaculture Layer (top) with created Reference Aquaculture Layer (bottom) for the three target deltas assessed with Landsat SR data and time period from September 2014 to September 2016.

	YRD	PRD	RRD
Sentinel-1 Aquaculture Layer			
Number of ponds	19,070	264,894	61,289
Total aquaculture pond area (km^2)	828.6	1,050.7	299.4
Reference Aquaculture Layer			
Number of detected ponds	15,270	169,194	30,915
Number of detected ponds (%)	80.1	63.9	50.4
Total pond area detected (km^2)	791.2	853.1	238.6
Total pond area detected (%)	95.5	81.2	79.7

2.4.2 Mapping of the Aquaculture Dynamics

The dynamics of aquaculture for all four deltas were visualised with a colour-palette from blue (early in time) to dark red (late in time) with a corresponding grading in colour for each year, as can be seen in Figure 2.5–2.8. Each aquaculture pond was highlighted in the colour of the year of its first appearance. Therefore, the colours give no evidence about the duration of their existence or their persistence. The detailed map extents are not chosen systematically and serve for illustration purposes only. The maps provide an impression on general aquaculture characteristics, like pond size (small or big), pond shape (square, round or elongated) or pond location (at the coast, at the course of rivers or other surface waters). Furthermore, the maps reveal spatial and temporal patterns, like the moving from coastal to inner delta regions, the development of ponds around surface waters. Larger versions of the maps can be found in the appendix (Figure A.14, A.15, A.16 and A.17).

Figure 2.5, depicts the spatial-temporal aquaculture dynamics for the YRD for the time period 1984–2016. The size of the aquaculture ponds is comparatively big, as can also be observed in Table 2.2. The ponds are predominantly elongated but also squared. Within the whole delta, aquaculture aggregates rather at the coastal regions, in particular at the north and south coast. Some minor misclassification can be found for a small amount of ponds e.g. within the course of the river.

The aquaculture within the PRD is characterised by the smallest mean pond size among the investigated deltas, as can also be observed from Table 2.2 and the map for the PRD in Figure 2.6. The map shows the dynamics of aquaculture for the time period from 1990–2016, but due to insufficient data coverage the years 2010, 2012 and 2015 could not be included in the analysis. The shape of the ponds is elongated or square-shaped. The majority of aquaculture ponds concentrate along the branches of the river or along the coast. The detailed extent within the map shows aquaculture at one of the river mouths within the delta. This spatial detail shows very clearly how aquaculture development gradually expanded from the coast towards inland within the course of the observation period.

For the RRD, only five year (1990–1994, 1995–1999, 2000–2004, 2005–2009) and four year (2013–2016) intervals could be observed as a consequence of low data quality and quantity. Figure 2.7 shows a focus region of the delta. Most of the aquaculture within the delta is located at the coastline and at inner parts of the delta, fewer can be found close to the Red River. The mean aquaculture pond size is 4885 m^2 (Table 2.2) and, thus, comparable to the pond sizes within the PRD. The aquaculture ponds are rather in square shape than elongated. Just as in Figure 2.6, the detailed map extent of Figure 2.7 impressively shows how aquaculture development in the RRD expands from the coast towards inland.

The dynamics of aquaculture for the MRD are assessed on the basis of the GSW data set (Figure 2.8), as Landsat SR data were not available for this delta region. The first year of observation is 1989. Many of the aquaculture ponds already exist at that time, followed by a high amount of aquaculture ponds first appearing in the early 2000s. Furthermore, it can be seen that aquaculture ponds developed aggregated from 2010 onwards.

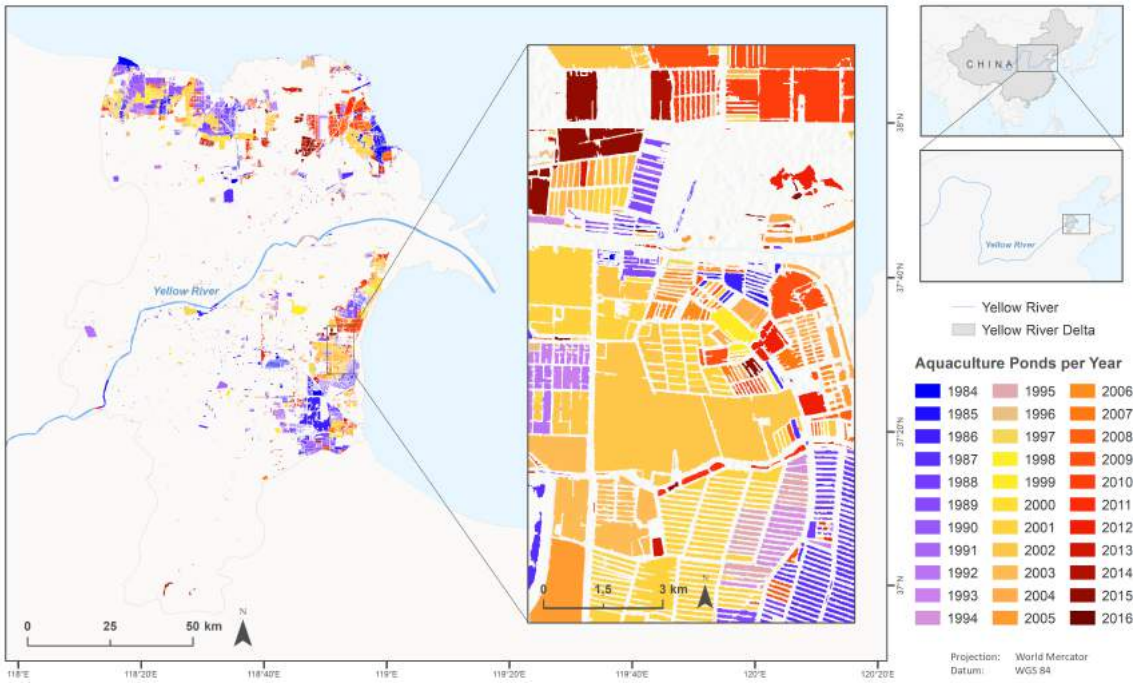

Figure 2.5: Aquaculture dynamics for the YRD from 1984–2016.

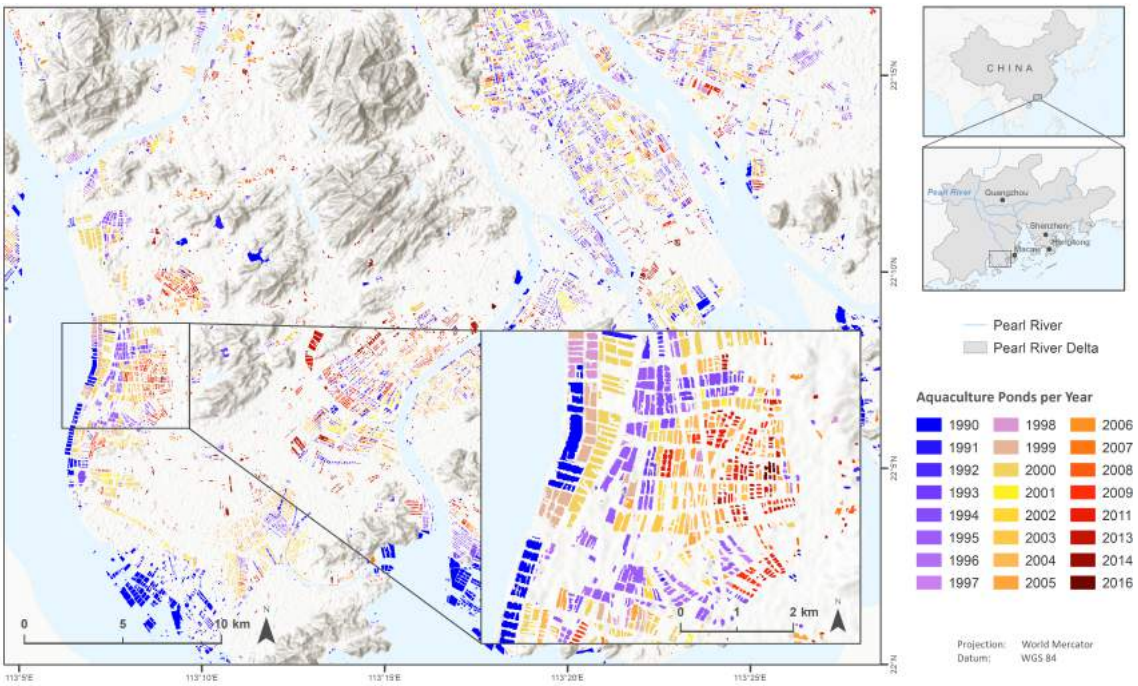

Figure 2.6: Aquaculture dynamics for the PRD from 1990–2016.

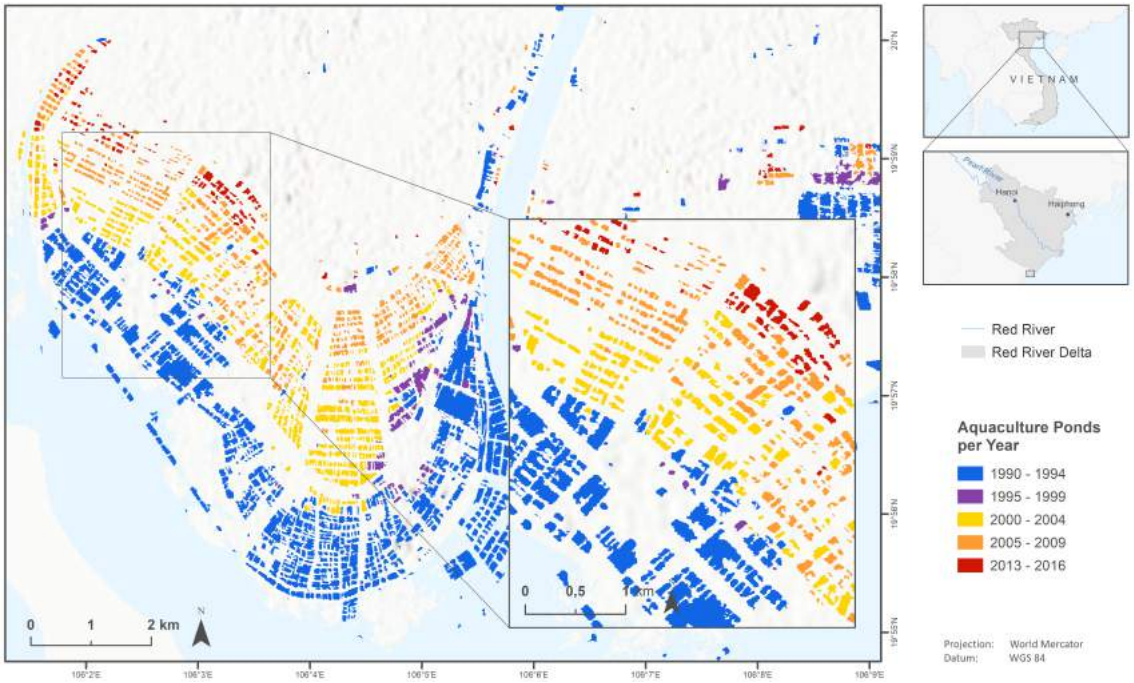

Figure 2.7: Aquaculture dynamics for the RRD from 1990–2016.

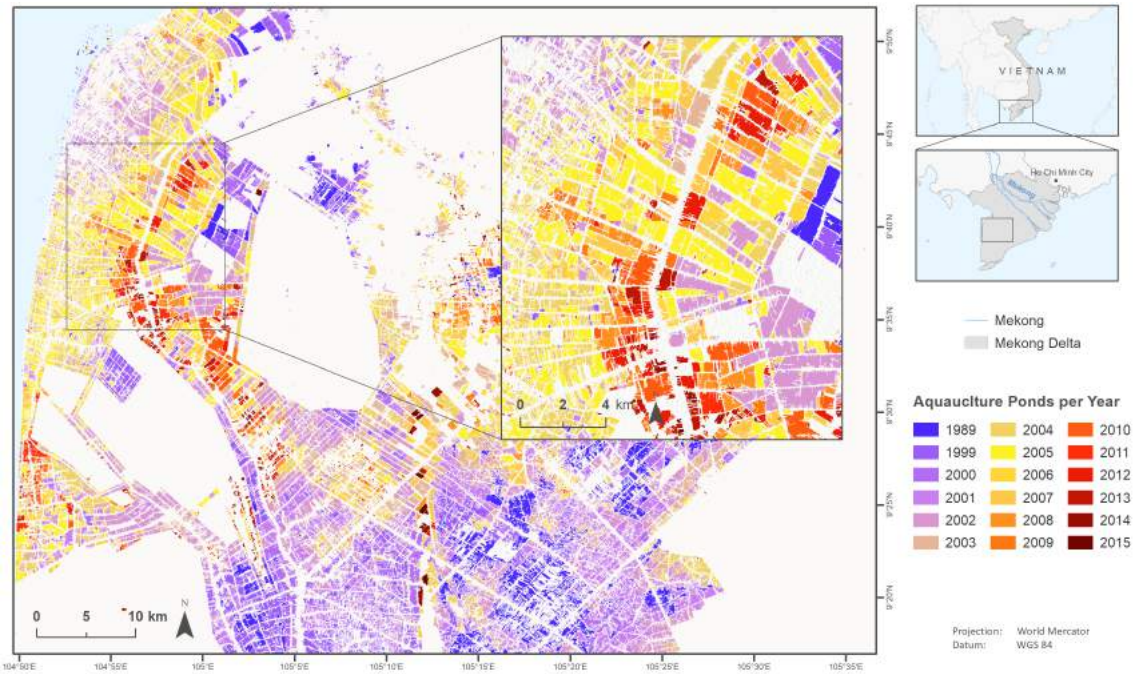

Figure 2.8: Aquaculture dynamics for the MRD from 1989–2015 based on the GSW dataset.

2.4.3 Quantification of Aquaculture Area

A comparison of the increase in aquaculture area obtained by Landsat SR and GSW data is shown in Table 2.4). The cumulative aquaculture area for the four delta regions can be seen in Figure 2.9. The bar graphs indicate the observed aquaculture area in km^2 within each delta for the years of investigation on the x-axis for the YRD (Landsat SR data: 1984–2016; GSW data: 1984–2015), the PRD (Landsat SR data: 1990–2016; GSW data: 1988–2015), the RRD (Landsat SR data: 1990–2016; GSW data: 1990–2015) and the MRD (1988–2015; analysed with GSW data only). Figure 2.10 shows separately the accompanied results from regression analyses with regression lines for each delta including the 95 % confidence region.

Based on Landsat SR data, different local peaks for the YRD can be seen for 1990 with 227 km^2, for 1998 with 278 km^2 and for 2002 with 434 km^2 (Figure 2.9). The maximum aquaculture area in this delta region occurred in year 2015 with 779 km^2. The minimum was observed for the year 1984 with a total aquaculture area of 42 km^2, which is also the beginning of the observation period. The Aquaculture area from 1984 to 2015, based on GSW data, shows also an increase although the overall increase is relatively low with 722 %, compared to the increase of 1856 % based on Landsat SR data (Table 2.4). At the beginning of the observation in 1984, the aquaculture area is calculated with 105 km^2 for the GSW data, which is a difference of approximately 63 km^2 compared to the assessment with Landsat data. In 2015 the aquaculture area is 807 km^2 for the GSW data, which corresponds to a difference of 27 km^2. However, a clear upward trend can be seen for both. The results from the regression analysis reveal that the annual increase in aquaculture area is identical for the YRD and amounts to 22 km^2 (Landsat SR data: adj. $R^2 = 0.95$, p-value = $<2.2 \times 10^{-16}$; GSW data set: adj. $R^2 = 0.91$, p-value = $<2.2 \times 10^{-16}$) (Figure 2.10).

Local peaks for the PRD can be detected for the assessment with Landsat data in 1993 with 364 km^2 and in 2008 with 664 km^2, whereas the maximum aquaculture area was observed in the year 2016 with 838 km^2, which marks the final year of the observation period. The overall minimum of aquaculture area for the PRD from 1990–2016 can be observed in 1991 with 187 km^2. The annual increase in aquaculture area assessed with Landsat data is 25 km^2 (adj. $R^2 = 0.91$, p-value = 2.64×10^{-10}) (Figure 2.10). Considering the aquaculture area for the PRD assessed with GSW data, an overall increase of 406 % from 241 km^2 to 674 km^2 in the period from 1988–2015 can be observed (Table 2.4). This coincides with an annual increase of 16 km^2 (adj. $R^2 = 0.75$, p-value = 5.362×10^{-7}). The annual increase is not in accordance with the results presented for the Landsat SR data, which revealed a 9 km^2 higher increase in aquaculture area per year (Figure 2.10). Therefore, the two different approaches provide dissimilar results for the temporal aquaculture dynamics in the PRD.

For the RRD, a continuous and steady increase in aquaculture can be observed from 132 km^2 in the 1990–1994 interval up to 205 km^2 observed for the 2013–2016 interval. On the basis of the GSW dataset, the areal increase for the RRD amounts to 16 km^2 for each multi-annual time step (adj. $R^2 = 0.73$, p-value = 0.04). Both assessments yield similar results for the RRD and show only slight differences. With the used GSW data, an aquaculture area of 136 km^2 for 1990–1994 and 197 km^2 for 2013–2015 is identified, which is an increase of 145 % (Figure 2.10). No significant trend can be revealed for the GSW data (adj. $R^2 = 0.73$, p-value = 0.06).

For the MRD, the surface area used for aquaculture increased from 352 km^2 in 1989 to 2507 km^2 in 2015, which corresponds to a total increase of 712 % (Figure 2.9). Therefore, the annual increase for the time period from 1989–2015 is 94 km^2 (adj. $R^2 = 0.74$, p-value $= 2.952 \times 10^{-6}$) per year (Figure 2.10). This is the highest yearly increase found within this study. Additionally, a strong increase can be observed from 1999–2005 and afterwards the area almost remains between 2200 km^2 and 2500 km^2.

Table 2.4: Increase in aquaculture area for the assessment based on Landsat SR data and GSW data showing the results for the first and last years of observation and accompanied increase in percent.

	Landsat SR data			GSW data		
	First year and aquaculture area (km^2)	Last year and aquaculture area (km^2)	Increase (%)	First year and aquaculture area (km^2)	Last year and aquaculture area (km^2)	Increase (%)
YRD	1984: 42	2016: 778	1856	1984: 105	2015: 807	722
PRD	1990: 207	2016: 839	406	1988: 241	2015: 674	279
RRD	1990-1994: 132	2013-2016: 205	155	1990-1994: 136	2013-2015: 197	145
MRD	–	–	–	1989: 352	2015: 2507	712

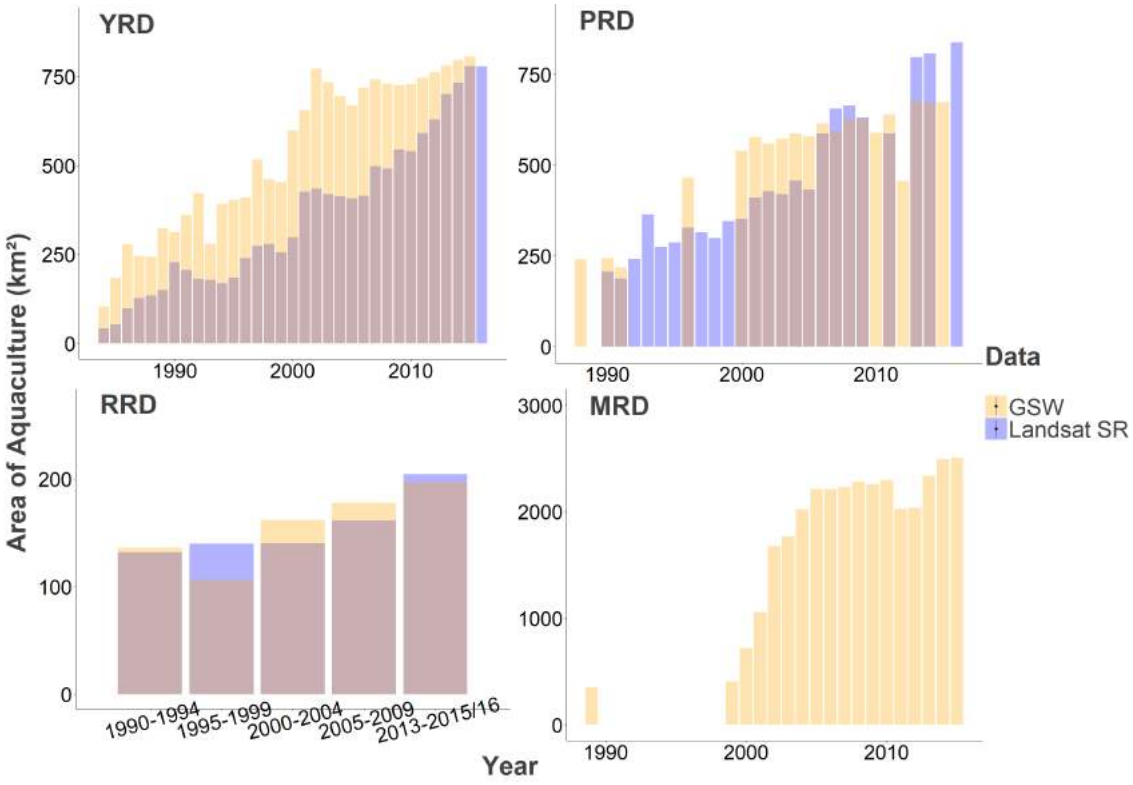

Figure 2.9: Cumulative aquaculture area for the YRD, PRD, RRD and MRD based on GSW data (yellow) and Landsat SR data (purple). The overlapping parts of the GSW data set and the Landsat SR are brownish coloured (mixture of both colours).

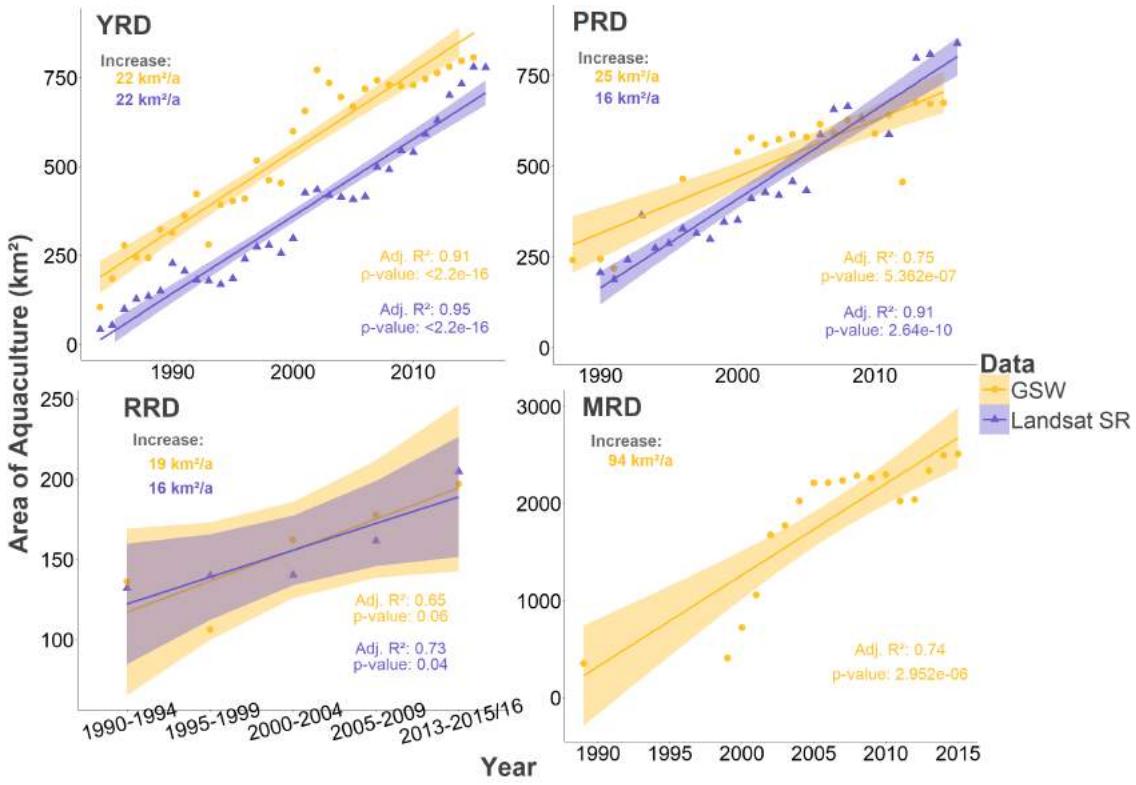

Figure 2.10: Trend in aquaculture area for the YRD, PRD, RRD and MRD based on GSW data (yellow) and Landsat SR data (purple) with adjusted R^2 and p-value obtained from the regression analysis. The overlapping parts of the GSW data set and the Landsat SR are brownish coloured (mixture of both colours).

2.4.4 Temporal Patterns and Hotspots

In order to reveal aquaculture patterns over time and to identify hotspot areas, a spatial explicit regression analysis was carried out for three deltas on the basis of the hexagon landscape (Figure 2.11, 2.12 and 2.13), described in Section 2.3.3. The maps reveal the trend of aquaculture development for the observed time period and for each 4000 m hexagon within the delta landscape (each hexagon area corresponds to approximately 13 million m^2). For areas without aquaculture no hexagons where generated. The observed trends are divided into four classes, namely increase in aquaculture area, decrease in aquaculture area, no observed trend or no significant change (p-value ≤ 0.05). The average increase in area of aquaculture per year or time step is again grouped according to the slope values retrieved from the regression analysis. The division into classes was made according to the Jenks' Natural Breaks algorithm (Jenks and Caspall, 1971) and the resulting values were rounded for reasons of clarity.

The map for the YRD can be seen in Figure 2.11. The delta is divided into a total of 494 hexagons containing aquaculture. Only 1.0 % of the hexagons show a decrease in aquaculture area and 9.7 % reveal no significant trend. For 441 hexagons, an increase in aquaculture area from 1984–2016 can be observed, which corresponds to 89.4 % of the total number of hexagons. For approximately 63 % of all hexagons (310 hexagons) aquaculture increase is <30,000 m^2). 8.5 % of the hexagons are characterised by high (180000–290,000 m^2) and very high (>290,000 m^2) increase per year. Considering the spatial distribution of these two classes and the medium increase

class (90000–180,000 m^2), the major increases of aquaculture over the considered time period are present at the coastline of the delta.

The PRD is divided into a total of 2,852 hexagons (Figure 2.12). 15.8 % of these showing no significant trend, 1.4 % revealing a declining trend in regard of aquaculture area and for 0.1 % no trend is apparent. The parts of the delta in which a decrease can be observed, are mainly located at the coastline or on offshore islands of the region. For 82.7 % of the hexagons an increase in aquaculture area from 1990–2016 can be observed. The high area increase classes (40000–80,000 m^2 and >80,000 m^2) are mostly located in near proximity to the Pearl River and can be found for some areas along the coast.

The spatio-temporal dynamics for aquaculture within the RRD is displayed in Figure 2.13. The whole region is divided into 1,003 hexagons of which 67.3 % reveal to be not significant, 0.9 % show no trend and 9.4 % show a decrease in aquaculture area over time. The remaining part of 22.4 % of the delta expose an increasing trend in aquaculture area. Although, the results of the regression analysis gave no significant results for most of the parts, the increase of aquaculture area at the coasts gives an idea on the patterns over time. The parts of the delta with declining trend are distributed all over the delta. Thus, no clear pattern can be revealed for the RRD.

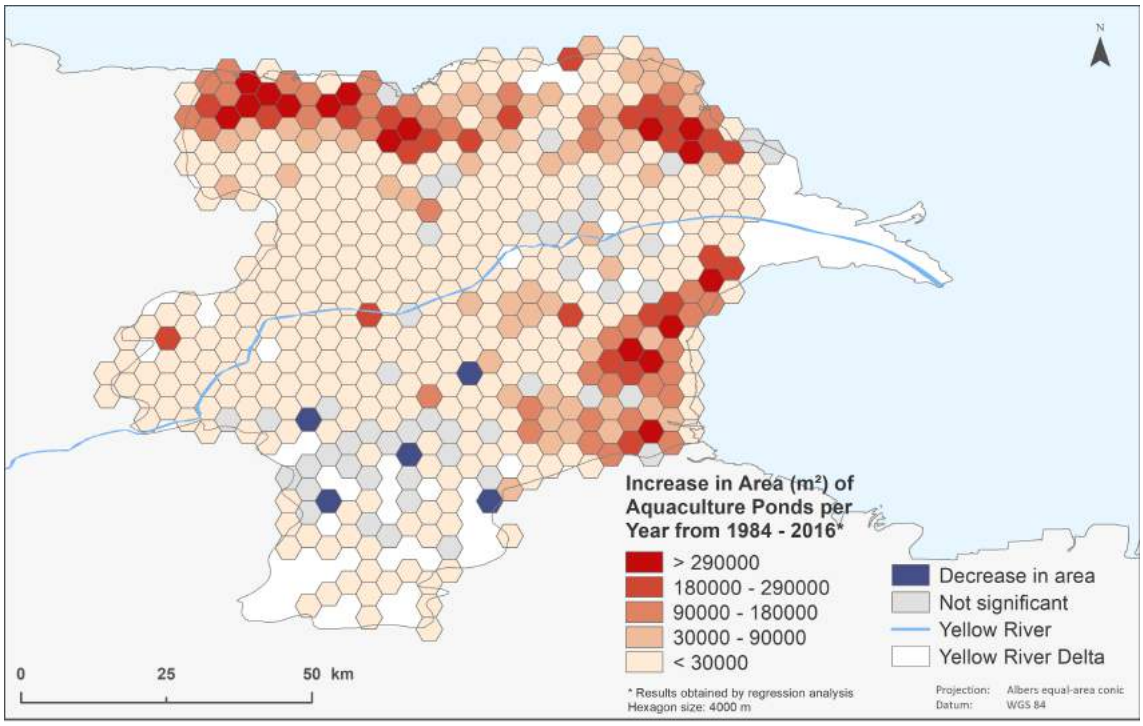

Figure 2.11: Temporal patterns and Hotspots of aquaculture expansion for the YRD.

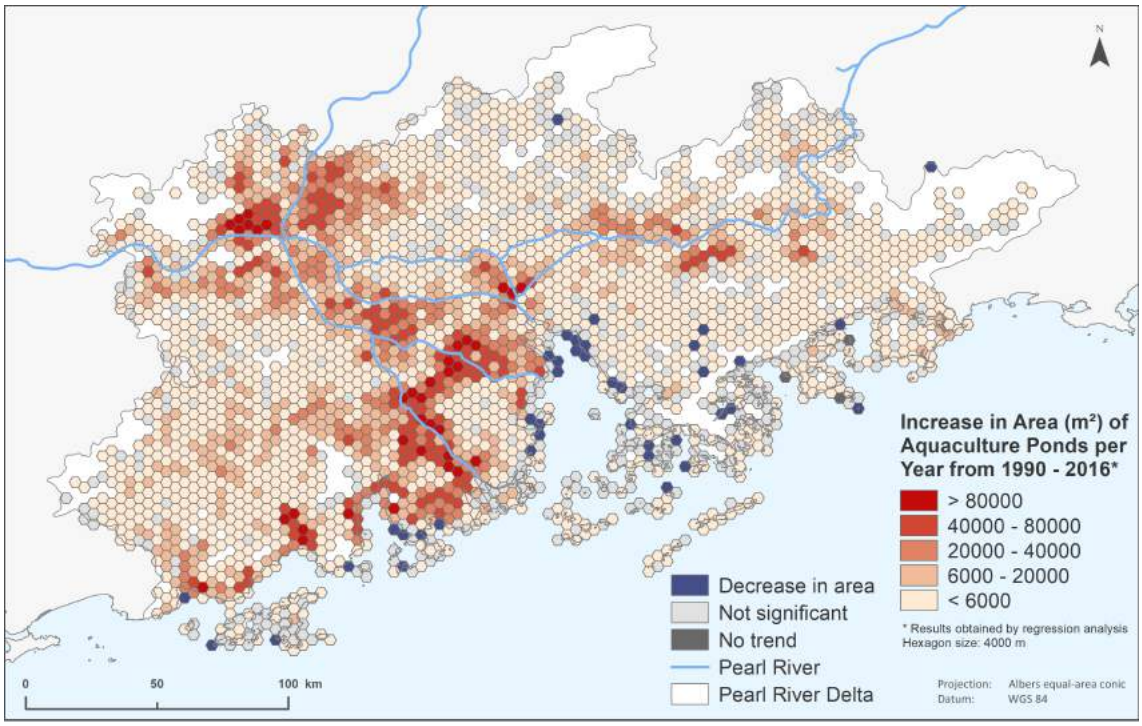

Figure 2.12: Temporal patterns and Hotspots of aquaculture expansion for the PRD.

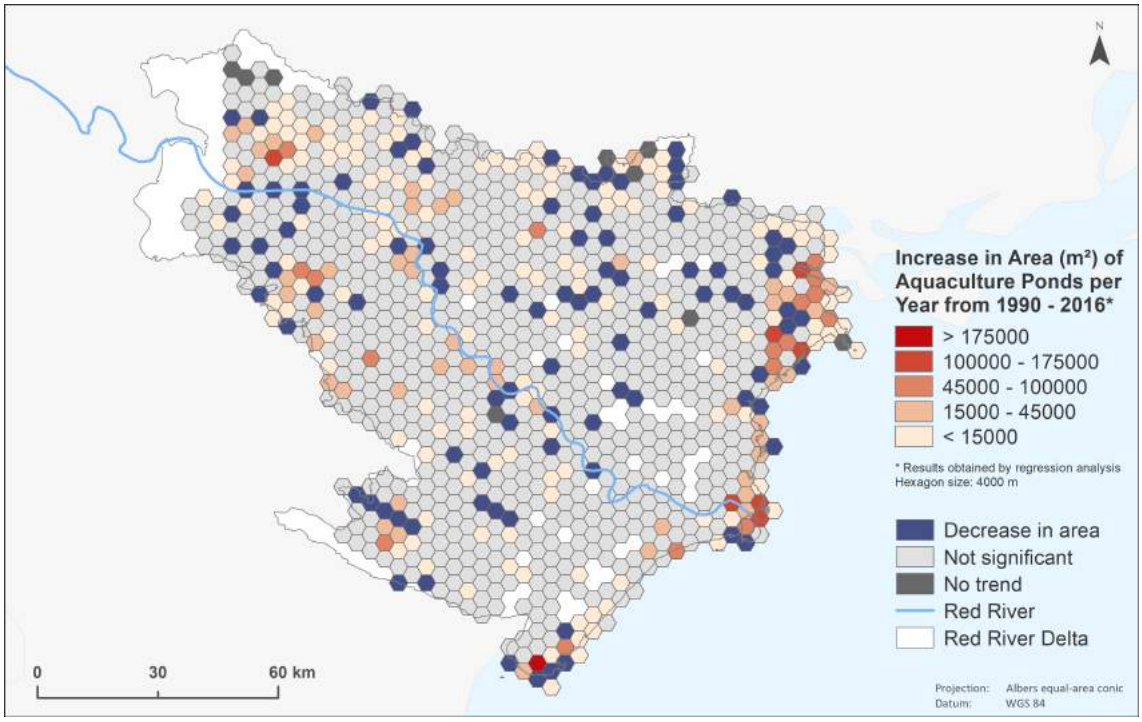

Figure 2.13: Temporal patterns and Hotspots of aquaculture expansion for the RRD.

2.4.5 Accuracy Assessment

The PRD serves exemplary for validating the outcomes of this study. The confusion matrix reveals, that a large majority was correctly identified as the class stable aquaculture with 196 aquaculture ponds out of 200, and, only 4 ponds were incorrectly assigned to this class (Table 2.5). However, only 88 aquaculture ponds were correctly classified as the class aquaculture change and 112 ponds were incorrectly detected as aquaculture change. Therefore, based on the presented approach, the class stable aquaculture is often confused with the class aquaculture change.

The accuracies and Kappa coefficient can be observed in Table 2.6. The Overall accuracy is given with 0.71 and represents the agreement of the prediction and the reference data. The computed Kappa with 0.72 can be categorised as a substantial agreement of both, prediction and reference data (Landis and Koch, 1977). The producer's accuracy is 0.64 for the class stable aquaculture and 0.95 for the class aquaculture change. The User's Accuracy is given with 0.98 for stable aquaculture and 0.56 for aquaculture change.

Table 2.5: Confusion matrix of the accuracy assessment for the PRD. The class stable aquaculture represents aquaculture ponds which are present in 2016 and present in a reference year in the past. The class aquaculture change account for aquaculture ponds which are present in 2016, however, not present in a reference year in the past. Following years were considered as reference years: 2014, 2011, 2008, 2006, 2005 and 2004.

		Reference		
		stable aquaculture	aquaculture change	Total
Prediction	stable aquaculture	196	4	200
	aquaculture change	112	88	200
	Total	308	92	400

Table 2.6: Accuracies and Kappa obtained by the accuracy assessment for the PRD.

Producer's Accuracy		**User's Accuracy**		**Overall Accuracy**	**Kappa**
stable aquaculture	aquaculture change	stable aquaculture	aquaculture change		
0.64	0.95	0.98	0.56	0.71	0.72

One source of error of this approach are ponds that have been converted from permanent, mostly natural, water bodies. These ponds are generally identified as aquaculture throughout the entire observation period regardless of their actual time point of conversion. Therefore, the proportions of permanent water bodies were quantified to have an idea on the impact of these water surfaces on the overall accuracy of this approach. The assessment of natural water bodies is shown in Table 2.7. For the YRD, 6.7 % of all ponds are identified as natural water surfaces which coincides with

3.8 % of the total aquaculture area. For the PRD, 3.9 % of the aquaculture ponds from the Reference Aquaculture Layer are considered to be natural water, which corresponds to 7.9 % of aquaculture area. 3.6 % of aquaculture ponds and 4.7 % of aquaculture area are detected as natural waters within the RRD.

Table 2.7: Assessment of natural water bodies within the target deltas. The shown numbers are in percentage of the total aquaculture ponds from the Reference Aquaculture Layer.

	Yellow River Delta	Pearl River Delta	Red River Delta
Number of ponds (%)	6.7	3.9	3.6
Area of ponds (%)	3.8	7.9	4.7

2.5 Discussion

2.5.1 Increase in Aquaculture Area

One major aim of this study was to investigate the change in aquaculture area within the observed time period for the target river deltas. The expectation was to observe an increase in area. An expansion in aquaculture area was revealed for each of the four deltas and for both assessments, based on Landsat SR data and based on the GSW data set.

Considering the assessment based on Landsat SR data, the highest relative and total increase was detected for the YRD (18.6-fold increase in aquaculture area from 1984 to 2016), although it is the smallest region of interest. This is in accordance with findings showing that the Shandong province is the main aquaculture producer along China's coastal regions (Gao et al., 2008). Furthermore, aquaculture is a major expanding land cover type within the YRD (Higgins et al., 2013; Ottinger et al., 2013). Another factor which might contribute to aquaculture expansion is the large size of single aquaculture ponds within the YRD (Table 2.2), which adds a high amount of aquaculture area per year caused by comparatively few additional ponds. The size of aquaculture ponds also supports that the aquaculture production in the YRD is rather commercial than on small household or subsistence scale (Hamilton, 2013). Based on the assessment with the GSW data set, the increase in aquaculture area deviates substantially from the results based on Landsat SR data. The GSW results revealed a 7.1-fold increase in area (1984–2015) for the YRD, thereby increases in aquaculture area are considerably lower. Water areas might be overestimated for the beginning of the observation period, which would cause the overall increase in aquaculture area to be lower. Large areas at the coast have been identified as water, e.g. seasonally flooded land cover types like wetlands and floodplains. This effect has also been shown during the creation of water masks, whereby water surfaces were especially overrepresented along the coast of the YRD, which resulted in bigger water areas for the coastal regions (Figure A.18).

The PRD is characterised by a 4.1-fold increase based on Landsat data and a 2.8-fold increase based on the GSW data set (Table 2.4). The magnitude of aquaculture expansion is again lower for the assessment with GSW data set and can be justified based on the assumption made in the previous paragraph. The increase in aquaculture area is relatively low for the PRD, when compared to the findings for

the YRD. This might be caused by rapid urban growth within the Pearl delta region. In the past decades, a major part of the delta's former agriculture area has been turned into building land for real estate and industry (Li and Yeh, 2004; Zhou and Sun, 2010). As a consequence, it is no longer available for aquaculture production. In addition, the PRD became the biggest urban region in size and population (World Bank Group, 2015), which rather promotes urbanisation than increases in aquaculture area. Although the total increase in aquaculture area is lower for the PRD, its expansion in area of 632 km^2 (Landsat SR data) and 279 km^2 (GSW data set) is considerable with an annual increase in area of approximately 25 km^2 (Landsat SR data) and 16 km^2 (GSW data set). This let to the conclusion, that aquaculture is still maintaining and increasing in area, even in the most populated urban region worldwide.

The aquaculture area in the RRD shows a 1.6-fold increase based on Landsat data and a 1.5-fold increase based on the assessment with GSW data set, indicating a solid agreement of both assessments for this delta region. The aquaculture expansion is comparatively low with 73 km^2 (Landsat SR data) and 61 km^2 (GSW data set) for the observation period. A possible reason can be found within the historical LULC change in Vietnam. As stated earlier, the Vietnamese renovation reforms were enacted in 1986, followed by mangrove removal and intensification of agriculture, also promoting excessive aquaculture expansion within the RRD in less than one decade (Seto and Fragkias, 2007). Consequently, major changes in aquaculture might have taken place prior to the first year of observation in 1990 and, thus, are not considered within the observed time period. In addition, mangrove reforestation programs were initiated in 1988 and two nature reserves were established in 1988 and 1995, covering a total coastal area of 145 km^2 (Seto and Fragkias, 2007), which would not favour aquaculture expansion. Both circumstances might have contributed to the comparatively low increase in aquaculture area within the RRD.

A strong increase in aquaculture area is demonstrated for the MRD showing a 7.1-fold increase in aquaculture area from 1988 to 2015 and annual aquaculture expansion of 94 km^2 (GSW data set). Unfortunately, no comparison based on Landsat SR data can be drawn for the MRD, as data was not available for this delta region. The MRD is an important region for the Vietnamese agricultural sector, e.g. rice paddy production, and contributes enormous amounts of capture fisheries and aquaculture. Especially in the 1980s and 1990s mangrove forests were destroyed for aquaculture farming (Cosslett and Cosslett, 2014), which is also reflected in the substantial increase in aquaculture area found in this study. Comparing the expansion of capture fisheries and aquaculture between 2000 and 2010, aquaculture production increased much faster with an annual growth rate of 18.46 % compared to 9.88 % in capture fisheries (Cosslett and Cosslett, 2014). In addition, the production of aquaculture goods revealed a 5-fold increase from 2000 to 2010 (Cosslett and Cosslett, 2014). The strongest increase in aquaculture area was also shown for this time period with an approximately tripling of the aquaculture area (Figure 2.9). This indicates, that the increase in production is linked with an increase in aquaculture area, too.

To conclude, both assessments revealed that aquaculture dynamics are characterised by notable expansions of aquaculture area within the observed time period. From an economic point of view, an increase in aquaculture is likely to be followed by economic growth (Toufique and Belton, 2014), decrease in poverty (Irz et al.,

2007; Kaliba et al., 2007) and an increase in welfare on the individual basis (Pant et al., 2014). From a nature conservation point of view, increases in aquaculture area are linked with increasing ecological vulnerability of the delta regions ranging from salinisation (Pine and Boyd, 2011) over pollution (Li et al., 2009; Herbeck et al., 2013; He et al., 2016) to wetland change and mangrove removal (Xu et al., 2011; Pham and Yoshino, 2016; Richards and Friess, 2016). The results regarding aquaculture expansion revealed that the increase in aquaculture varies in terms of magnitude among the four deltas. In addition, aquaculture ponds structures, e.g. pond size, are very different for the investigated deltas, both facts emphasising that aquaculture management requires adaptable conservation strategies. As shrimp farming is a big contributor to Asian aquaculture production, but is also very hazardous for the environment (Cao et al., 2007), two general scenarios for sustainable shrimp aquaculture exist (Bush et al., 2010). These are designed for either small-scale producers or industrial scale producers (Bush et al., 2010), which could be applied based on delta-specific conditions. Moreover, several studies on optimising aquaculture farming exist. In general, low-intensity aquaculture has the potential to decrease environmental pressure. It could support the reproduction success for natural depleted populations, uses less feed and environmentally disturbing supplements (Diana, 2012) and can be integrated into coastal and mangrove habitats, while maintaining their ecological functions (Bush et al., 2010). Another option would be to promote plant-based aquaculture which has been shown to positively influence water quality by removing nutrients from coastal waters (Xiao et al., 2017) and from wastewaters originating during aquaculture production (Kumar et al., 2015).

2.5.2 Dynamics and Hotspots of Aquaculture

No clear hotspot patterns could be revealed for the RRD, as the regression analysis was not significant, which might be a result of the low amount of data input (1990–1994, 1995–1999, 2000–2004, 2005–2009 and 2013–2016). However, the example result map for the RRD (Figure 2.7) revealed a spatio-temporal pattern of aquaculture expansion developing from coast towards inland, arguing that aquaculture was first located at the coast and with growth in production new aquaculture ponds have been built at the inner part of the coast.

For the YRD and the PRD, clear trends in hotspots of aquaculture expansion have been revealed (Figure 2.11 and Figure 2.12). Hotspots have been expected to be located at the coast and along the river course of the deltas, mainly due to easy water supply. This hypothesis has been validated, although with remarkable differences among the two deltas.

Hotspots of aquaculture expansion within the YRD have been detected along the coast. This is in accordance with findings from Ottinger et al. (2013), who found increases in cultivated aquatic surfaces primarily in coastal areas. Additionally, the authors stated that aquaculture expansion is characterised by a coastward movement with strongest increases in area within 3–5 km from the coastline in 2010, which coincides with the results of this study. Aquaculture is often found in coastal areas as coasts provide easy access to water resources and they belong to low lying regions which are favourable for aquaculture production (Primavera, 2006).

On the contrary, for the PRD, the hotspots of aquaculture increase are located along the course of the river (Figure 2.12). In the PRD, aquaculture is traditionally

located along the river as farmers can easily fill up ponds with freshwater from the river (Ruddle and Zhong, 1988). Consequently, this pattern is still apparent and the findings assume that additional aquafarms have been created along the Pearl River during the observed period. Simultaneously, several areas along the coast have been detected to show a decrease in aquaculture from 1990–2016. This might be a consequence of urban land expansion, as the PRD is characterised by major urbanisation processes and by industrial growth (Zhao et al., 2017). This also causes considerable water pollution with heavy metals (Nguyen van et al., 2016). As water for aquaculture farming is mainly withdrawn from the Pearl River, the polluted water within the aquaculture ponds is absorbed by the farmed aquatic species. The heavy metals can be detected in cultured fish (Nghia et al., 2009; Cheng et al., 2013), therefore, heavy metal contamination can be considered as a public health concern (Liang et al., 2016).

To sum up, hotspots of aquaculture expansion were found to be mainly located along the coast (YRD) and rivers (PRD). Especially in Chinese delta regions water quality is poor (Li et al., 2009; Liang et al., 2016; Wohlfart et al., 2016). In aquaculture farming, it is common practice to discharge polluted water unfiltered (Ottinger et al., 2016). Therefore, it can be assumed that increase in aquaculture production in the investigated deltas is contributing to a deterioration of water quality.

2.5.3 Potentials and Limitations of This Study

The outcomes of this study revealed the increases of aquaculture within all target regions and illustrated the hotspots of aquaculture expansion for two deltas. However, several limitations need to be taken into consideration regarding the methods and assumptions used.

The Landsat archive provides an outstanding availability of free EO imagery covering a long-term time period (Wulder et al., 2012). To exploit this data source, Landsat SR data have been used to identify spatio-temporal dynamics of aquaculture over the last decades. However, optical satellite data are vulnerable to the effects of clouds, thus, are restricted for applications in cloud-prone areas, such as the humid tropics (Asner, 2001). This was observable when processing data for the RRD, experiencing missing data for many years. This was also true for some years within the observed time period for the PRD. High cloud coverage influenced the quality of annual composites, which might be an explanation for the annual fluctuations within the results for the aquaculture area (Figure 2.9). Additionally, no Landsat SR data were available for the MRD. Therefore, data quality and availability were major constraints of this study. Nevertheless, the presented results provide an overview on the general trends in aquaculture expansion and give insights in the aquaculture dynamics and the hotspot development.

Another limitation for detecting the water areas of aquaculture with Landsat imagery is the coarse spatial resolution of 30 m. A high proportion of aquaculture ponds from the Sentinel-1 Aquaculture Layer were not able to be detected with used Landsat SR data (Table 2.3). Therefore, aquaculture area might be considerably higher than observed by this study. In addition, the outcomes of the accuracy assessment showed, that aquaculture ponds have often been failed to be detected for the past years (Table 2.6 and 2.5). A major reason to be named is the coarse spatial resolution of Landsat imagery, as large ponds in the YRD were more suit-

able for being detected than smaller aquaculture ponds of the PRD and the RRD. Therefore, aquaculture characterised by bigger ponds is more likely to be detected than aquaculture consisting of rather small ponds. That might also be caused by pixel-mixing effects (Birnie, 1986), which make it difficult to identify smaller aquaculture ponds. However, it does also make a difference which type of aquaculture is observed. Alexandridis et al. (2008) compared different imagery on the application of the identification of marine mussel farms and argue that high resolution imagery does not automatically give the best results for aquaculture assessments, and the sensor types should be chosen according to observed aquaculture type.

Furthermore, all assessments of this study are based on the Sentinel-1 Aquaculture Layer. Thus, it is assumed that aquaculture ponds did not change for the observed time period, which would indicate a bias in the results. The used Sentinel-1 Aquaculture Layer is based on the aquaculture pond location and extent for the time period from September 2014 to September 2016. This would also lead in biggest aquaculture area for this period based on the assessment with Landsat SR data. Therefore, aquaculture area for the last years of observation might be overrepresented, whereas aquaculture ponds in former times are not considered and might be underestimated. Based on the accuracy assessment, it was revealed that aquaculture ponds in the past have almost ever been correctly classified as aquaculture ponds. However, based on the prediction data –representing the assessment based on this approach– aquaculture ponds have not been detected in 56 % of the cases (Table 2.6). This argues, that more aquaculture ponds have been present in the past and were not detected by this approach, indicating that aquaculture area was underestimated at that point of time and therefore, the expansion of aquaculture might be overestimated for the observation period.

In addition, the approach ignores the presence of other water features like natural waters. These water features were not excluded within the analysis. Therefore, natural waters which have been turned into aquaculture during the observation period, are a source of error. Especially along the coasts of the PRD, additional aquaculture ponds have been built in natural coastal floodplains, in the sea (by extending the coastline) (Figure A.19) or in inland waters in the RRD (Figure A.20). However, this error was quantified by assessing natural water bodies for the first years of observation (1984 for the YRD, 1990 for the PRD and 1990–1994 for the RRD). The results showed that this effect does matter for aquaculture within the observed target deltas with 3.8 % of aquaculture area accounting for natural waters within the YRD, 7.9 % for the PRD and 4.7 % for the RRD (Table 2.7). As a consequence, the presence of natural waters affected the analysis of aquaculture and, furthermore, might also influence the hotspot patterns found for the YRD and the PRD. Therefore, I suggest to eliminate natural waters before assessing changes in aquaculture in further research. One option would be to manually extract them based on the GSW data set. Another option is to apply the presented approach by Han et al. (2005), which is based on feature extraction methods using Landsat imagery enabling the separation of aquaculture from other water features. However, it can be doubt that this can accurately be performed for single aquaculture ponds solely on the basis of Landsat data and would require imagery with higher spatial resolution (Ottinger et al., 2017), which might not be available for a deltawide or continentwide assessment.

Besides stated limitations of this study, an overall accuracy of 71 % and a substantial Kappa coefficient of 0.72 were shown for the used temporal metrics (Table 2.6). These results reveal a thorough accuracy for the presented approach. Furthermore, spatio-temporal dynamics and patterns of aquaculture of four river deltas have been detected, also highlighting similarities and differences among the deltas. The approach itself can easily be applied on larger spatial scales, either by using Landsat SR data or with the help of global datasets like the used GSW product. The approach is not site-specific, therefore, suitable for being used in other target regions. Although it requires a high resolution aquaculture layer comparable to the Sentinel-1 Aquaculture Layer, Ottinger et al. (2017) state that it can easily be created for other regions even on continental and global scales. Within this study, the combination of the Sentinel-1 Aquaculture Layer with Landsat data guaranteed for precise mapping of the aquaculture ponds and opened the possibility to exploit the long-term data availability of the Landsat fleet. The combination of radar and Landsat satellite data are widely used in the field of EO, where radar data has been shown to be a valuable complementary data source to Landsat imagery (Shimabukuro et al., 2007; Eckardt et al., 2013; Cheng et al., 2016), which was also demonstrated in this study.

2.5.4 Outlook

The presented findings revealed strong increases in aquaculture area for all four river deltas. These results serve exemplary for other coastal regions in Asia and highlight major environmental impacts of such a development. As Asia has become the leading global aquaculture producer contributing almost 90 % of quantity, further increases in aquaculture area have to be expected. This is particularly hazardous for the sensitive coastal ecosystems, as many environmental consequences of aquaculture expansion are already present and are likely to intensify in the future. Based on the investigated deltas, the findings of this study suggest that aquaculture expansion is not following equal spatio-temporal dynamics. Therefore, unique management efforts need to be elaborated to guarantee for human welfare and ecosystem functioning.

Following up the results of this study, an assessment for the complete Asian coast would be the next step in further research. Based on this, the detection of spatio-temporal dynamics for the coastal areas would not be restricted to single delta regions, but showing aquaculture development for the entire coastal regions of Asia. Therefore, similarities and differences of delta versus non-delta regions could be retrieved, also highlighting the strongest increases in aquaculture area over time along the Asian coastal zone and revealing possible indicators for the development of aquaculture expansions and dynamics. This could also be compared for conservation areas versus non-conservation areas or wetland areas versus non-wetland areas, which would have valuable implications for the management of coastal regions across Asia.

References

Alexandridis, T. K., Topaloglou, C. A., Lazaridou, E., and Zalidis, G. C. The performance of satellite images in mapping aquacultures. *Ocean & Coastal Management*, 51(8-9): 638–644, 2008. doi:10.1016/j.ocecoaman.2008.06.002.

Almonacid-Caballer, J., Pardo-Pascual, J., and Ruiz, L. Evaluating fourier cross-correlation sub-pixel registration in Landsat images. *Remote Sensing*, 9(10):1–15, 2017. doi:10.3390/rs9101051.

Alonso-Pérez, F., Ruiz-Luna, A., Turner, J., Berlanga-Robles, C. A., and Mitchelson-Jacob, G. Land cover changes and impact of shrimp aquaculture on the landscape in the Ceuta coastal lagoon system, Sinaloa, Mexico. *Ocean & Coastal Management*, 46 (6-7):583–600, 2003. doi:10.1016/S0964-5691(03)00036-X.

Arneth, A., Sitch, S., Pongratz, J., Stocker, B. D., Ciais, P., Poulter, B., Bayer, A. D., Bondeau, A., Calle, L., Chini, L. P., Gasser, T., Fader, M., Friedlingstein, P., Kato, E., Li, W., Lindeskog, M., Nabel, J. E. M. S., Pugh, T. A. M., Robertson, E., Viovy, N., Yue, C., and Zaehle, S. Historical carbon dioxide emissions caused by land-use changes are possibly larger than assumed. *Nature Geoscience*, 10(2):79–84, 2017. ISSN 1752-0894. doi:10.1038/ngeo2882.

Asner, G. P. Cloud cover in Landsat observations of the Brazilian Amazon. *International Journal of Remote Sensing*, 22(18):3855–3862, 2001. ISSN 0143-1161. doi:10.1080/01431160010006926.

Barsi, J., Lee, K., Kvaran, G., Markham, B., and Pedelty, J. The spectral response of the Landsat-8 Operational Land Imager. *Remote Sensing*, 6(12):10232–10251, 2014. doi:10.3390/rs61010232.

Béland, M., Goïta, K., Bonn, F., and Pham, T. T. H. Assessment of land–cover changes related to shrimp aquaculture using remote sensing data: A case study in the Giao Thuy District, Vietnam. *International Journal of Remote Sensing*, 27(8):1491–1510, 2006. ISSN 0143-1161. doi:10.1080/01431160500406888.

Bellwood, P. S. *First farmers: The origins of agricultural societies*. Blackwell Pub, Malden, MA, 2007. ISBN 978-0-631-20565-4.

Berlanga-Robles, C. A., Ruiz-Luna, A., Bocco, G., and Vekerdy, Z. Spatial analysis of the impact of shrimp culture on the coastal wetlands on the northern coast of Sinaloa, Mexico. *Ocean & Coastal Management*, 54(7):535–543, 2011. doi:10.1016/j.ocecoaman.2011.04.004.

Birnie, R. V. Pixel-mixing effects and their significance to identifying snow condition from Landsat MSS data. *International Journal of Remote Sensing*, 7(7):845–853, 1986. ISSN 0143-1161. doi:10.1080/01431168608948894.

Bocquet-Appel, J.-P. When the world's population took off: The springboard of the Neolithic Demographic Transition. *Science*, 333(6042):560–561, 2011. doi:10.1126/science.1208880.

Bui, T. D., Maier, S. W., and Austin, C. M. Land cover and land use change related to shrimp farming in coastal areas of Quang Ninh, Vietnam using remotely sensed data. *Environmental Earth Sciences*, 72(2):441–455, 2014. ISSN 1866-6280. doi:10.1007/s12665-013-2964-0.

Bush, S. R., van Zwieten, P. A., Visser, L., van Dijk, H., Bosma, R., de Boer, W. F., and Verdegem, M. Scenarios for resilient shrimp aquaculture in tropical coastal areas. *Ecology and Society*, 15(2):1–17, 2010. ISSN 1708-3087. doi:10.5751/ES-03331-150215.

Cao, L., Wang, W., Yang, Y., Yang, C., Yuan, Z., Xiong, S., and Diana, J. Environmental impact of aquaculture and countermeasures to aquaculture pollution in China. *Environmental Science and Pollution Research - International*, 14(7):452–462, 2007. ISSN 0944-1344. doi:10.1065/espr2007.05.426.

Cheng, Y., Le Yu, Cracknell, A. P., and Gong, P. Oil palm mapping using Landsat and PALSAR: A case study in Malaysia. *International Journal of Remote Sensing*, 37(22): 5431–5442, 2016. ISSN 0143-1161. doi:10.1080/01431161.2016.1241448.

Cheng, Z., Man, Y. B., Nie, X. P., and Wong, M. H. Trophic relationships and health risk assessments of trace metals in the aquaculture pond ecosystem of Pearl River Delta, China. *Chemosphere*, 90(7):2142–2148, 2013. ISSN 1879-1298. doi:10.1016/j.chemosphere.2012.11.017.

Cohen, J. A coefficient of agreement for nominal scales. *Educational and Psychological Measurement*, 20(1):37–46, 1960. ISSN 0013-1644. doi:10.1177/001316446002000104.

Cosslett, T. L. and Cosslett, P. D. *Water Resources and Food Security in the Vietnam Mekong Delta*, volume 44 of *Natural Resource Management and Policy*. Springer, Switzerland, 2014. ISBN 978-3-319-02197-3.

Cui, Y., Liu, J., Hu, Y., Wang, J., and Kuang, W. Modeling the radiation balance of different urban underlying surfaces. *Chinese Science Bulletin*, 57(9):1046–1054, 2012. ISSN 1001-6538. doi:10.1007/s11434-011-4933-x.

Diana, J. S. Aquaculture production and biodiversity conservation. *BioScience*, 59(1): 27–38, 2009. ISSN 1525-3244. doi:10.1525/bio.2009.59.1.7.

Diana, J. S. Is lower intensity aquaculture a valuable means of producing food? An evaluation of its effects on near-shore and inland waters. *Reviews in Aquaculture*, 4(4): 234–245, 2012. ISSN 17535123. doi:10.1111/j.1753-5131.2012.01079.x.

Eckardt, R., Berger, C., Thiel, C., and Schmullius, C. Removal of optically thick clouds from multi-spectral satellite images using multi-frequency SAR data. *Remote Sensing*, 5(12):2973–3006, 2013. doi:10.3390/rs5062973.

European Commission. Global Surface Water Explorer, 2016. URL `https://global-surface-water.appspot.com/`.

Falcucci, A., Maiorano, L., and Boitani, L. Changes in land-use/land-cover patterns in Italy and their implications for biodiversity conservation. *Landscape Ecology*, 22(4): 617–631, 2007. ISSN 0921-2973. doi:10.1007/s10980-006-9056-4.

FAO. *The State of World Fisheries and Aquaculture 2016: Contributing to food security and nutrition for all*. The state of world fisheries and aquaculture. Rome, 2016. ISBN 978-92-5-109185-2.

Foga, S., Scaramuzza, P. L., Guo, S., Zhu, Z., Dilley, R. D., Beckmann, T., Schmidt, G. L., Dwyer, J. L., Joseph Hughes, M., and Laue, B. Cloud detection algorithm comparison and validation for operational Landsat data products. *Remote Sensing of Environment*, 194:379–390, 2017. ISSN 00344257. doi:10.1016/j.rse.2017.03.026.

Gao, J., Yang, Z., and Xie, J. Review on demand, markets and trade of farming fishery products in China, 2008.

Garibaldi, L. The fao global capture production database: A six-decade effort to catch the trend. *Marine Policy*, 36(3):760–768, 2012. doi:10.1016/j.marpol.2011.10.024.

General Statistic Office of Vietnam, 2015. URL https://gso.gov.vn/Default_en.aspx?tabid=491.

Gibbs, H. K., Ruesch, A. S., Achard, F., Clayton, M. K., Holmgren, P., Ramankutty, N., and Foley, J. A. Tropical forests were the primary sources of new agricultural land in the 1980s and 1990s. *Proceedings of the National Academy of Sciences of the United States of America*, 107(38):16732–16737, 2010. ISSN 1091-6490. doi:10.1073/pnas.0910275107.

Gorelick, N., Hancher, M., Dixon, M., Ilyushchenko, S., Thau, D., and Moore, R. Google Earth Engine: Planetary-scale geospatial analysis for everyone. *Remote Sensing of Environment*, 202:18–27, 2017. ISSN 00344257. doi:10.1016/j.rse.2017.06.031.

Ha, T. P., Dieperink, C., van Dang Tri, P., Otter, H. S., and Hoekstra, P. Governance conditions for adaptive freshwater management in the Vietnamese Mekong Delta. *Journal of Hydrology*, 557:116–127, 2018. ISSN 00221694. doi:10.1016/j.jhydrol.2017.12.024.

Hamilton, S. Assessing the role of commercial aquaculture in displacing mangrove forest. *Bulletin of Marine Science*, 89(2):585–601, 2013. ISSN 00074977. doi:10.5343/bms.2012.1069.

Han, J., Chi KwangHoon, and Yeon YeonKwang. Aquaculture feature extraction from satellite image using independent component analysis. In Perner Petra and Imiya Atsushi, editors, *Machine Learning and Data Mining in Pattern Recognition*, pages 660–666. Springer, Berlin, Heidelberg, 2005. ISBN 978-3-540-26923-6.

Hardy, R. W. Utilization of plant proteins in fish diets: Effects of global demand and supplies of fishmeal. *Aquaculture Research*, 41(5):770–776, 2010. doi:10.1111/j.1365-2109.2009.02349.x.

He, Z., Cheng, X., Kyzas, G. Z., and Fu, J. Pharmaceuticals pollution of aquaculture and its management in China. *Journal of Molecular Liquids*, 223:781–789, 2016. ISSN 01677322. doi:10.1016/j.molliq.2016.09.005.

Herbeck, L. S., Unger, D., Wu, Y., and Jennerjahn, T. C. Effluent, nutrient and organic matter export from shrimp and fish ponds causing eutrophication in coastal and back-reef waters of NE Hainan, tropical China. *Continental Shelf Research*, 57:92–104, 2013. ISSN 02784343. doi:10.1016/j.csr.2012.05.006.

Higgins, S., Overeem, I., Tanaka, A., and Syvitski, J. P. M. Land subsidence at aquaculture facilities in the Yellow River delta, China. *Geophysical Research Letters*, 40(15):3898–3902, 2013. ISSN 00948276. doi:10.1002/grl.50758.

Irz, X., Stevenson, J. R., Tanoy, A., Villarante, P., and Morissens, P. The equity and poverty impacts of aquaculture: Insights from the Philippines. *Development Policy Review*, 25(4):495–516, 2007. ISSN 09506764. doi:10.1111/j.1467-7679.2007.00382.x.

Jenks, G. F. and Caspall, F. C. Error on chorophlethic maps: definition, measurement, reduction. *Annals of the Association of American Geographers*, 61(2):217–244, 1971. ISSN 0004-5608. doi:10.1111/j.1467-8306.1971.tb00779.x.

Jetz, W., Wilcove, D. S., and Dobson, A. P. Projected impacts of climate and land-use change on the global diversity of birds. *PloS Biology*, 5(6):1211–1219, 2017. doi:10.1371/journal.pbio.0050157.g001.

Kaliba, A. R., Ngugi, C. C., Mackambo, J. M., Osewe, K. O., Senkondo, E., Mnembuka, B. V., and Amisah, S. Potential effect of aquaculture promotion on poverty reduction in Sub-Saharan Africa. *Aquaculture International*, 15(6):445–459, 2007. ISSN 0967-6120. doi:10.1007/s10499-007-9110-5.

Ke, C.-Q., Zhang, D., Wang, F.-Q., Chen, S.-X., Schmullius, C., Boerner, W.-M., and Wang, H. Analyzing coastal wetland change in the Yancheng National Nature Reserve, China. *Regional Environmental Change*, 11(1):161–173, 2011. ISSN 1436-3798. doi:10.1007/s10113-010-0130-8.

Keesing, J. K., Liu, D., Fearns, P., and Garcia, R. Inter- and intra-annual patterns of Ulva prolifera green tides in the Yellow Sea during 2007-2009, their origin and relationship to the expansion of coastal seaweed aquaculture in China. *Marine pollution bulletin*, 62 (6):1169–1182, 2011. ISSN 1879-3363. doi:10.1016/j.marpolbul.2011.03.040.

Khorram, S., Nelson, S. A., Koch, F. H., and van der Wiele, C. F. *Remote Sensing*. Springer-Verlag New York, Boston, MA, 1 edition, 2012. ISBN 978-1-4614-3103-9. doi:10.1007/978-1-4614-3103-9.

Kumar, D., Santhanam, P., Thillainayagam, J., Kumar, N., Selvaraju, A., Devi, S., and Prasath, B. Excessive nutrients and heavy metals removal from diverse wastewaters using marine microalga Chlorella marina (Butcher). *Indian Journal of Geo-Marine Sciences*, 44:97–103, 2015.

Landis, J. R. and Koch, G. G. The measurement of observer agreement for categorical data. *Biometrics*, 33(1):159–174, 1977. doi:10.2307/2529310.

Lee, J. H., Pang, I.-C., Moon, I.-J., and Ryu, J.-H. On physical factors that controlled the massive green tide occurrence along the southern coast of the Shandong Peninsula in 2008: A numerical study using a particle-tracking experiment. *Journal of Geophysical Research*, 116:1–12, 2011. ISSN 0148-0227. doi:10.1029/2011JC007512.

Li, H. Y., Man, W. D., Li, X. Y., Ren, C. Y., Wang, Z. M., Li, L., Jia, M. M., and Mao, D. H. Remote sensing investigation of anthropogenic land cover expansion in the low-elevation coastal zone of Liaoning Province, China. *Ocean & Coastal Management*, 148: 245–259, 2017. doi:10.1016/j.ocecoaman.2017.08.007.

Li, X. and Yeh, A. G.-O. Analyzing spatial restructuring of land use patterns in a fast growing region using remote sensing and GIS. *Landscape and Urban Planning*, 69(4): 335–354, 2004. ISSN 01692046. doi:10.1016/j.landurbplan.2003.10.033.

Li, X., Mander, Ü., Ma, Z., and Jia, Y. Water quality problems and potential for wetlands as treatment systems in the Yangtze River Delta, China. *Wetlands*, 29(4):1125–1132, 2009. ISSN 0277-5212. doi:10.1672/08-205.1.

Liang, P., Wu, S.-C., Zhang, J., Cao, Y., Yu, S., and Wong, M.-H. The effects of mariculture on heavy metal distribution in sediments and cultured fish around the Pearl River Delta region, south China. *Chemosphere*, 148:171–177, 2016. ISSN 1879-1298. doi:10.1016/j.chemosphere.2015.10.110.

Masek, J. G., Vermote, E. F., Saleous, N. E., Wolfe, R., Hall, F. G., Huemmrich, K. F., Gao, F., Kutler, J., and Lim, T.-K. A Landsat Surface Reflectance dataset for North America, 1990–2000. *IEEE Geoscience and Remote Sensing Letters*, 3(1):68–72, 2006. doi:10.1109/LGRS.2005.857030.

McFeeters, S. K. The use of the Normalized Difference Water Index (NDWI) in the delineation of open water features. *International Journal of Remote Sensing*, 17(7): 1425–1432, 1996. ISSN 0143-1161. doi:10.1080/01431169608948714.

Myers, N., Mittermeier, R. A., Mittermeier, C. G., da Fonseca, Gustavo A. B., and Kent, J. Biodiversity hotspots for conservation priorities. *Nature*, 403(6772):853–858, 2000. ISSN 1476-4687. doi:10.1038/35002501.

Naylor, R. L., Goldburg, R. J., Primavera, J. H., Kautsky, N., Beveridge, M. C., Clay, J., Folke, C., Lubchenco, J., Mooney, H., and Troell, M. Effect of aquaculture on world fish supplies. *Nature*, 405(6790):1017–1024, 2000. ISSN 1476-4687. doi:10.1038/35016500.

Nghia, N. D., Lunestad, B. T., Trung, T. S., Son, N. T., and Maage, A. Heavy metals in the farming environment and in some selected aquaculture species in the Van Phong Bay and Nha Trang Bay of the Khanh Hoa Province in Vietnam. *Bulletin of environmental contamination and toxicology*, 82(1):75–79, 2009. ISSN 1432-0800. doi:10.1007/s00128-008-9561-z.

Nguyen, T. S., Chen, C.-F., Chang, N.-B., Chen, C.-R., Chang, L.-Y., and Thanh, B.-X. Mangrove mapping and change detection in Ca Mau Peninsula, Vietnam, using Landsat data and object-based image analysis. *IEEE Journal of Selected Topics in Applied Earth Observations and Remote Sensing*, 8(2):503–510, 2015. ISSN 1939-1404. doi:10.1109/JSTARS.2014.2360691.

Nguyen van, T., Ozaki, A., Nguyen Tho, H., Nguyen Duc, A., Tran Thi, Y., and Kurosawa, K. Arsenic and heavy metal contamination in soils under different land use in an estuary in northern Vietnam. *International journal of environmental research and public health*, 13(11):1–13, 2016. ISSN 1660-4601. doi:10.3390/ijerph13111091.

Ottinger, M., Kuenzer, C., Liu, G., Wang, S., and Dech, S. Monitoring land cover dynamics in the Yellow River Delta from 1995 to 2010 based on Landsat 5 TM. *Applied Geography*, 44:53–68, 2013. ISSN 01436228. doi:10.1016/j.apgeog.2013.07.003.

Ottinger, M., Clauss, K., and Kuenzer, C. Aquaculture: Relevance, distribution, impacts and spatial assessments: A review. *Ocean & Coastal Management*, 119:244–266, 2016. doi:10.1016/j.ocecoaman.2015.10.015.

Ottinger, M., Clauss, K., and Kuenzer, C. Large-scale assessment of coastal aquaculture ponds with Sentinel-1 time series data. *Remote Sensing*, 9(5):1–23, 2017. doi:10.3390/rs9050440.

Pant, J., Barman, B. K., Murshed-E-Jahan, K., Belton, B., and Beveridge, M. Can aquaculture benefit the extreme poor? A case study of landless and socially marginalized Adivasi (ethnic) communities in Bangladesh. *Aquaculture*, 418-419:1–10, 2014. ISSN 00448486. doi:10.1016/j.aquaculture.2013.09.027.

Pattanaik, C. and Narendra Prasad, S. Assessment of aquaculture impact on mangroves of Mahanadi delta (Orissa), East coast of India using remote sensing and GIS. *Ocean & Coastal Management*, 54(11):789–795, 2011. doi:10.1016/j.ocecoaman.2011.07.013.

Pauly, D. and Zeller, D. Catch reconstructions reveal that global marine fisheries catches are higher than reported and declining. *Nature communications*, 7:1–9, 2016. ISSN 2041-1723. doi:10.1038/ncomms10244.

Pauly, D. and Zeller, D. Comments on FAOs state of world fisheries and aquaculture (SOFIA 2016). *Marine Policy*, 77:176–181, 2017. doi:10.1016/j.marpol.2017.01.006.

Pekel, J.-F., Cottam, A., Gorelick, N., and Belward, A. S. High-resolution mapping of global surface water and its long-term changes. *Nature*, 540(7633):418–422, 2016. ISSN 1476-4687. doi:10.1038/nature20584.

Peneva-Reed, E. Understanding land-cover change dynamics of a mangrove ecosystem at the village level in Krabi Province, Thailand, using Landsat data. *GIScience & Remote Sensing*, 51(4):403–426, 2014. ISSN 1548-1603. doi:10.1080/15481603.2014.936669.

Pettorelli, N., Schulte to Bühne, H., Tulloch, A., Dubois, G., Macinnis-Ng, C., Queirós, A. M., Keith, D. A., Wegmann, M., Schrodt, F., Stellmes, M., Sonnenschein, R., Geller, G. N., Roy, S., Somers, B., Murray, N., Bland, L., Geijzendorffer, I., Kerr, J. T., Broszeit, S., Leitão, P. J., Duncan, C., El Serafy, G., He, K. S., Blanchard, J. L., Lucas, R., Mairota, P., Webb, T. J., Nicholson, E., Rowcliffe, M., and Disney, M. Satellite remote sensing of ecosystem functions: Opportunities, challenges and way forward. *Remote Sensing in Ecology and Conservation*, 112(3):1–23, 2017. ISSN 20563485. doi:10.1002/rse2.59.

Pham, T. D. and Yoshino, K. Impacts of mangrove management systems on mangrove changes in the Northern Coast of Vietnam. *Tropics*, 24(4):141–151, 2016. doi:10.3759/tropics.24.141.

Phiri, D. and Morgenroth, J. Developments in Landsat land cover classification methods: A review. *Remote Sensing*, 9(967):1–25, 2017. doi:10.3390/rs9090967.

Pine, H. J. and Boyd, C. E. Stream salinization by inland brackish-water aquaculture. *North American Journal of Aquaculture*, 73(2):107–113, 2011. ISSN 1522-2055. doi:10.1080/15222055.2011.545580.

Primavera, J. H. Overcoming the impacts of aquaculture on the coastal zone. *Ocean & Coastal Management*, 49(9-10):531–545, 2006. doi:10.1016/j.ocecoaman.2006.06.018.

Rajitha, K., Mukherjee, C. K., Vinu Chandran, R., and Prakash Mohan, M. M. Land-cover change dynamics and coastal aquaculture development: A case study in the East Godavari delta, Andhra Pradesh, India using multi-temporal satellite data. *International Journal of Remote Sensing*, 31(16):4423–4442, 2010. ISSN 0143-1161. doi:10.1080/01431160903277456.

Ren, M. Sediment discharge of the Yellow River, China: Past, present and future-A synthesis. *Acta Oceanologica Sinica*, 34(2):1–8, 2015. doi:10.1007/s13131-015-0619-6.

Richards, D. R. and Friess, D. A. Rates and drivers of mangrove deforestation in Southeast Asia, 2000-2012. *Proceedings of the National Academy of Sciences of the United States of America*, 113(2):344–349, 2016. ISSN 1091-6490. doi:10.1073/pnas.1510272113.

Ruddle, K. and Zhong, G. *Integrated agriculture-aquaculture in south China. The dike-pond system of the Zhujiang Delta.* Cambridge University Press, Cambridge, UK, 1988. ISBN 978-0521341936.

Sala, O. E., Chapin III, F. S., Armesto, J. J., Berlow, E., Bloomfield, J., Dirzo, R., Huber-Sanwald, E., Huenneke, L. F., Jackson, R. B., Kinzig, A., Leemans, R., Lodge, D. M., Mooney, H. A., Oesterheld, M., Poff, N. L., Sykes, M. T., Walker, B. H., Walker, M., and Wall, D. H. Global biodiversity scenarios for the year 2100. *Science*, 287(5459): 1770–1774, 2000. doi:10.1126/science.287.5459.1770.

Seto, K. C. and Fragkias, M. Mangrove conversion and aquaculture development in Vietnam: A remote sensing-based approach for evaluating the Ramsar Convention on Wetlands. *Global Environmental Change*, 17:486–500, 2007. ISSN 09593780. doi:10.1016/j.gloenvcha.2007.03.001.

Shimabukuro, Y. E., Almeida-Filho, R., Kuplich, T. M., and de Freitas, R. M. Quantifying optical and SAR image relationships for tropical landscape features in the Amazônia. *International Journal of Remote Sensing*, 28(17):3831–3840, 2007. ISSN 0143-1161. doi:10.1080/01431160701236829.

Stotz, W. When aquaculture restores and replaces an overfished stock: Is the conservation of the species assured? The case of the scallop Argopecten purpuratus in Northern Chile. *Aquaculture International*, 8:237–247, 2000. doi:10.1023/A:1009215119051.

Toufique, K. A. and Belton, B. Is aquaculture pro-poor? Empirical evidence of impacts on fish consumption in Bangladesh. *World Development*, 64:609–620, 2014. doi:10.1016/j.worlddev.2014.06.035.

Turner, W., Rondinini, C., Pettorelli, N., Mora, B., Leidner, A. K., Szantoi, Z., Buchanan, G., Dech, S., Dwyer, J., Herold, M., Koh, L. P., Leimgruber, P., Taubenboeck, H., Wegmann, M., Wikelski, M., and Woodcock, C. Free and open-access satellite data are key to biodiversity conservation. *Biological Conservation*, 182:173–176, 2015. ISSN 00063207. doi:10.1016/j.biocon.2014.11.048.

U.S. Geological Survey. Product guide: Landsat 8 Surface Reflectance Code (LaSRC) product: Version 4.2. URL `https://landsat.usgs.gov/sites/default/files/documents/lasrc_product_guide.pdf`.

Valiela, I., Bowen, J. L., and York, J. K. Mangrove forests: One of the world's threatened major tropical environments. *BioScience*, 51(10):807, 2001. ISSN 1525-3244. doi:10.1641/0006-3568(2001)051[0807:MFOOTW]2.0.CO;2.

Wang, S., Tang, D., He, F., Fukuyo, Y., and Azanza, R. V. Occurrences of harmful algal blooms (HABs) associated with ocean environments in the South China Sea. *Hydrobiologia*, 596(1):79–93, 2008. ISSN 0018-8158. doi:10.1007/s10750-007-9059-4.

Wohlfart, C., Kuenzer, C., Chen, C., and Liu, G. Social–ecological challenges in the Yellow River basin (China): a review. *Environmental Earth Sciences*, 75(13):179, 2016. ISSN 1866-6280. doi:10.1007/s12665-016-5864-2.

Woodcock, C. E., Allen, R., Anderson, M., Belward, A., Bindschadler, R., Cohen, W., Gao, F., Goward, S. N., Helder, D., Helmer, E., Nemani, R., Oreopoulos, L., Schott, J., Thenkabail, P. S., Vermote, E. F., Vogelmann, J., Wulder, M. A., and Wynne, R. Free access to Landsat imagery. *Science (New York, N.Y.)*, 320(5879):1011, 2008. ISSN 1095-9203. doi:10.1126/science.320.5879.1011a.

World Bank Group. *East Asia's Changing Urban Landscape: Measuring a Decade of Spatial Growth*. The World Bank, Washington, 2015. ISBN 978-1-4648-0363-5. doi:10.1596/978-1-4648-0363-5.

Wulder, M. A., Masek, J. G., Cohen, W. B., Loveland, T. R., and Woodcock, C. E. Opening the archive: How free data has enabled the science and monitoring promise of Landsat. *Remote Sensing of Environment*, 122:2–10, 2012. ISSN 00344257. doi:10.1016/j.rse.2012.01.010.

Xiao, X., Agusti, S., Lin, F., Li, K., Pan, Y., Yu, Y., Zheng, Y., Wu, J., and Duarte, C. M. Nutrient removal from Chinese coastal waters by large-scale seaweed aquaculture. *Scientific reports*, 7:1–6, 2017. ISSN 2045-2322. doi:10.1038/srep46613.

Xu, C., Sheng, S., Zhou, W., Cui, L., and Liu, M. Characterizing wetland change at landscape scale in Jiangsu Province, China. *Environmental monitoring and assessment*, 179(1-4):279–292, 2011. ISSN 0167-6369. doi:10.1007/s10661-010-1735-6.

Young, N. E., Anderson, R. S., Chignell, S. M., Vorster, A. G., Lawrence, R., and Evangelista, P. H. A survival guide to Landsat preprocessing. *Ecology*, 98(4):920–932, 2017. ISSN 0012-9658. doi:10.1002/ecy.1730.

Zhao, M., Derudder, B., and Huang, J. Polycentric development in China's mega-city regions, 2001-08: A comparison of the Yangtze and Pearl River Deltas. *Die Erde*, 148 (1):1–13, 2017. doi:10.12854/erde-148-26.

Zhou, Q. and Sun, B. Analysis of spatio-temporal pattern and driving force of land cover change using multi-temporal remote sensing images. *Science China Technological Sciences*, 53(S1):111–119, 2010. ISSN 1674-7321. doi:10.1007/s11431-010-3196-0.

Zhu, Z. and Woodcock, C. E. Object-based cloud and cloud shadow detection in Landsat imagery. *Remote Sensing of Environment*, 118:83–94, 2012. ISSN 00344257. doi:10.1016/j.rse.2011.10.028.

Appendix

Software and software packages used for reading the spatial data, processing it and determining aquaculture hotspots:

- ArcGIS 10.5.1
- dplyr 0.7.4
- ggplot2 2.2.1
- gridExtra 2.3
- lemon 0.3.1
- plyr 1.8.4
- QGIS 2.18.3
- R Studio 1.1.383
- rgdal 1.2.4
- scales 0.4.1
- sp 1.2.3

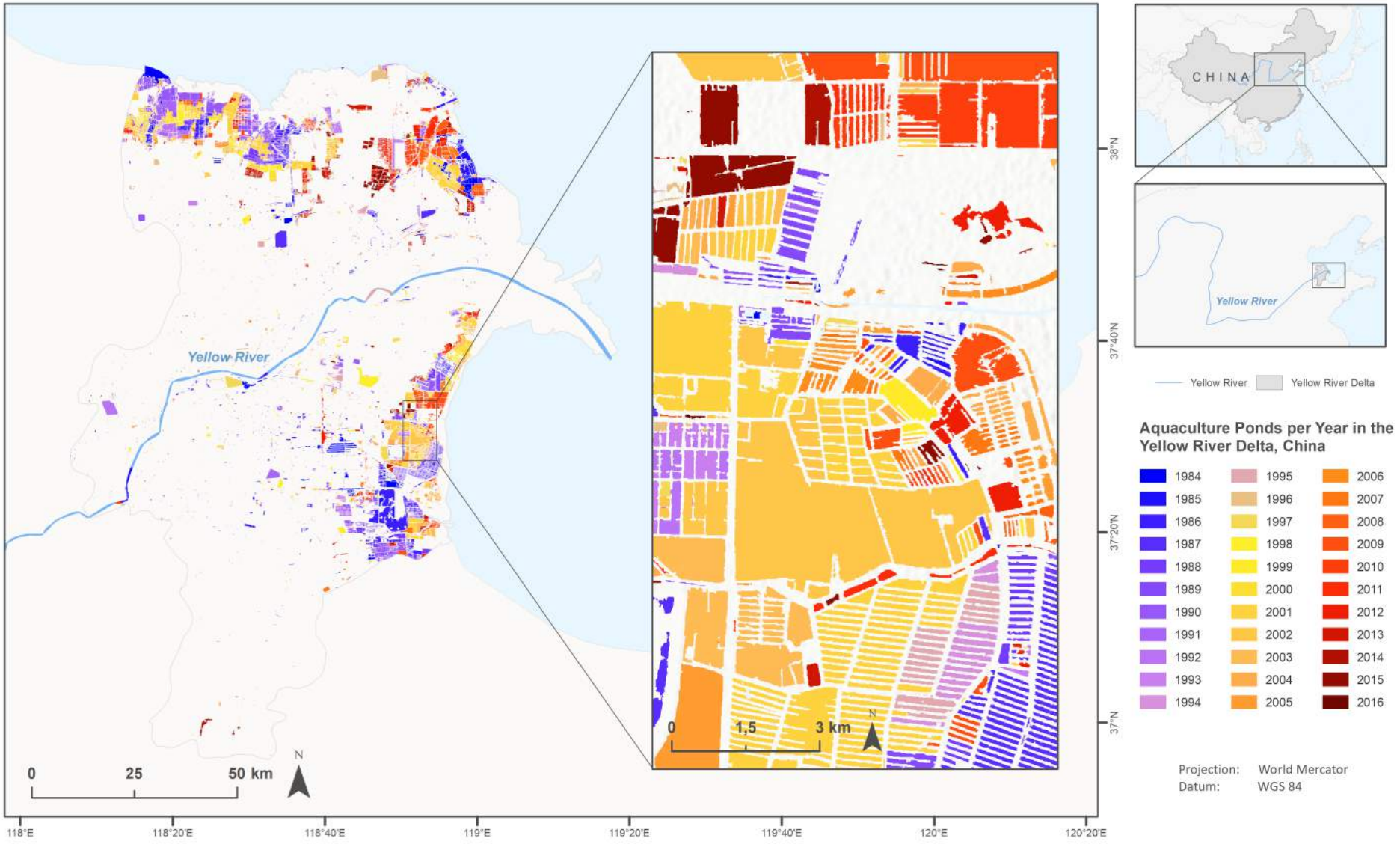

Figure A.14: Large map on the temporal patterns for the YRD.

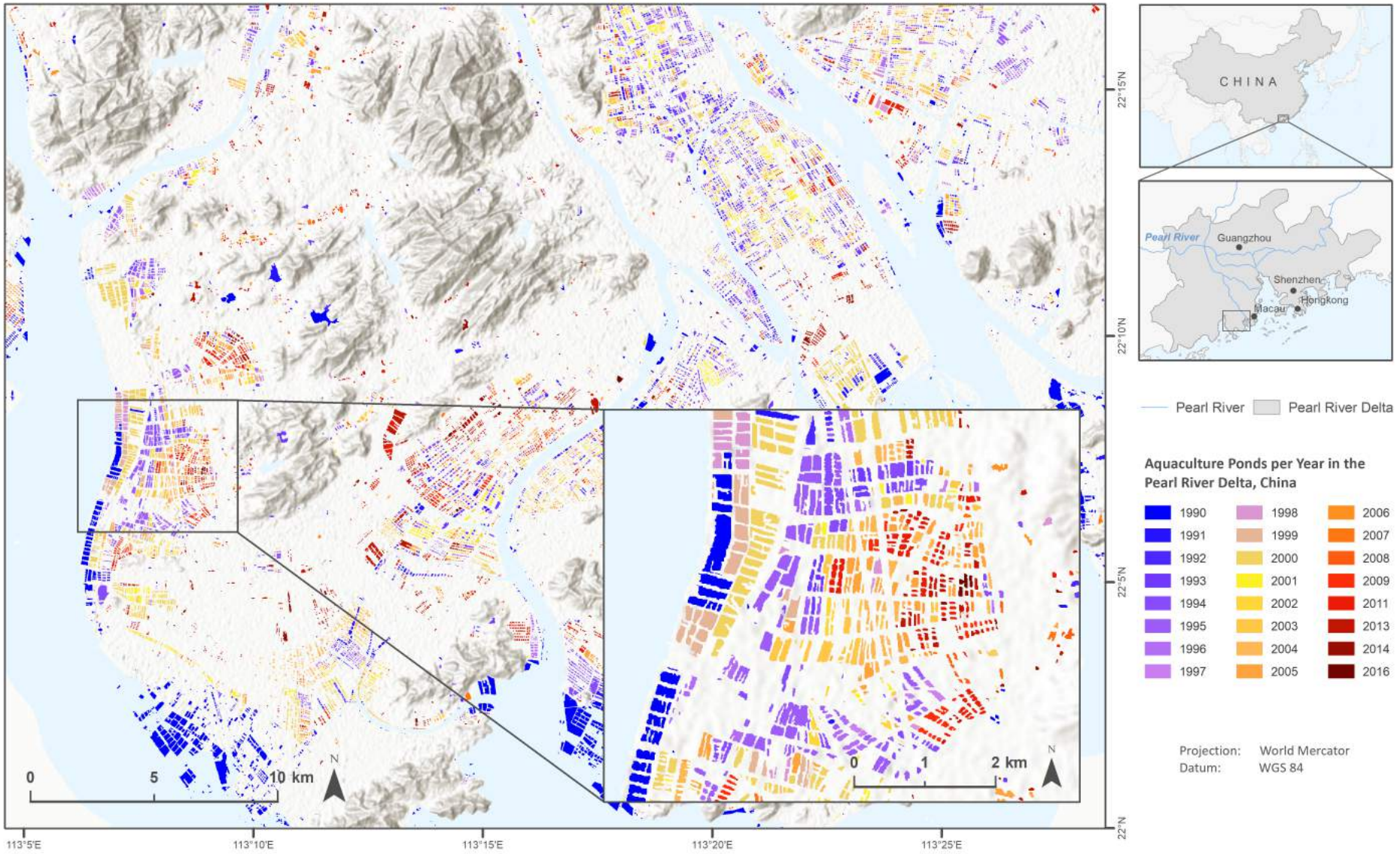

Figure A.15: Large map on the temporal patterns for the PRD.

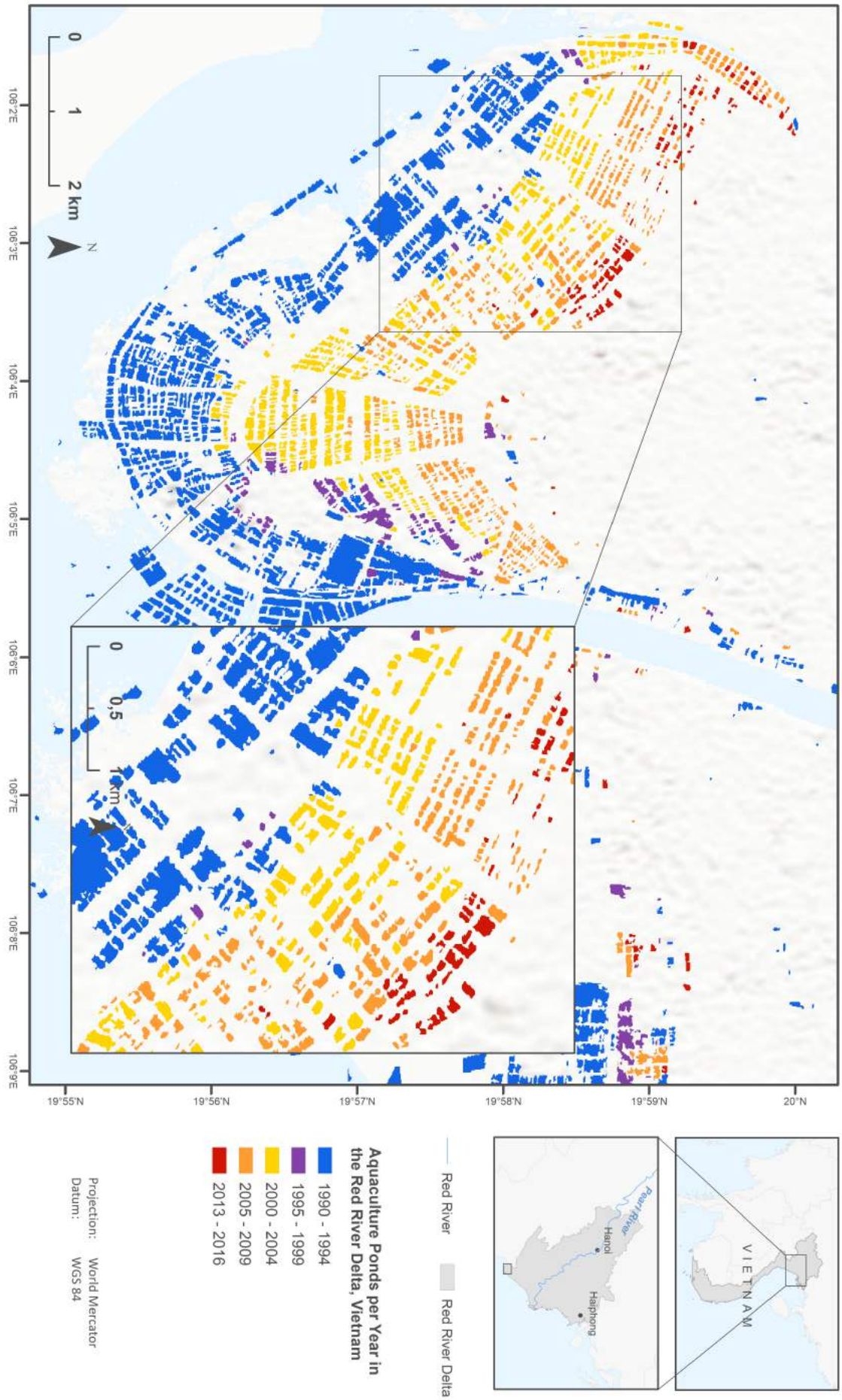

Figure A.16: Large map on the temporal patterns for the RRD.

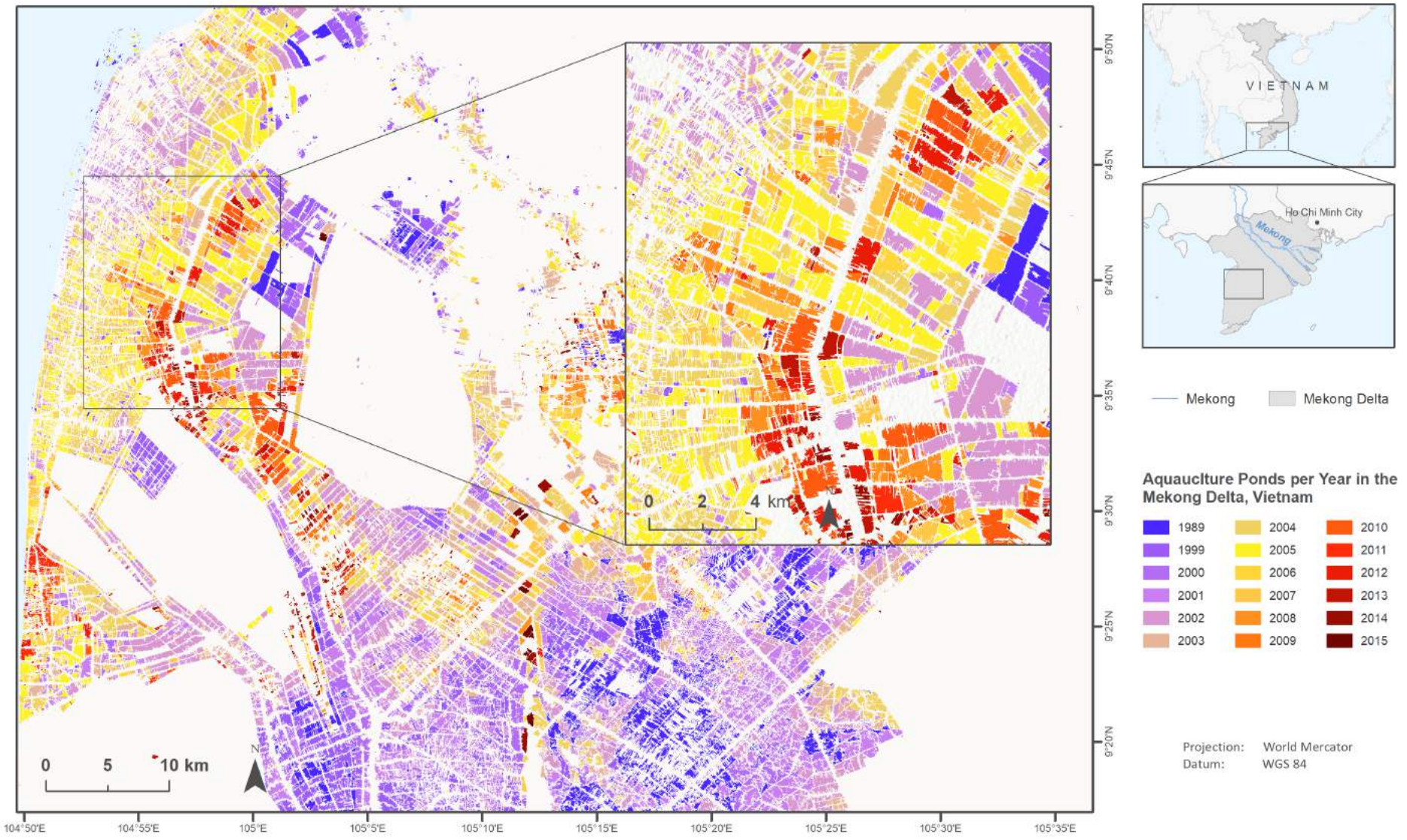

Figure A.17: Large map on the temporal patterns for the MRD.

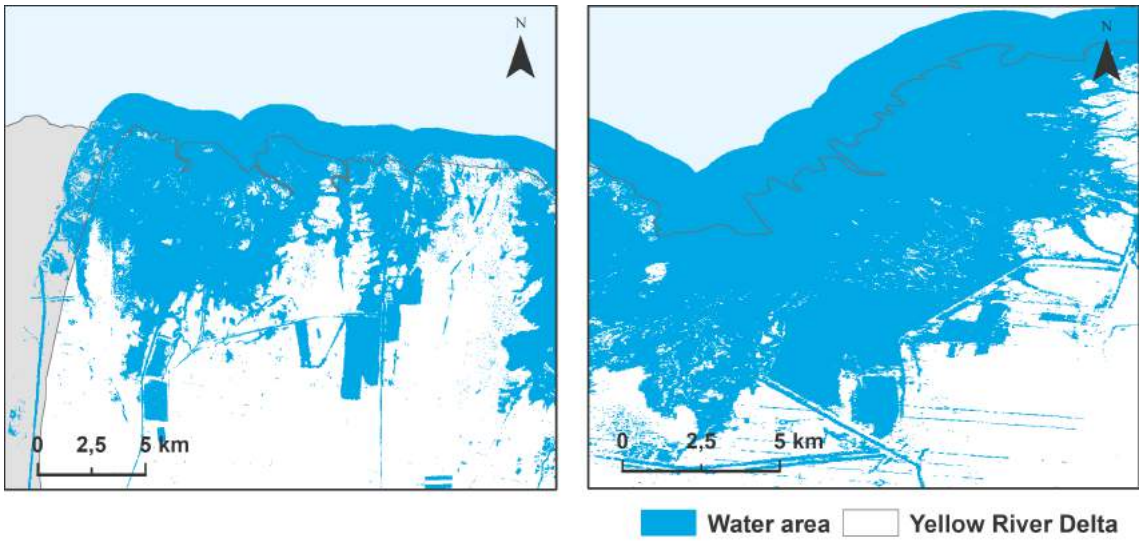

Figure A.18: Water areas retrieved from the GSW data. Both maps illustrate two parts of the binary water mask from the YRD for 1984 which is used for the validation assessment based on the GSW data. It can be seen that the water areas are large and a separation between single aquaculture ponds is not possible. This results in a higher aquaculture area for the initial year 1984 compared to the assessment based on Landsat SR data. This might be the reason for the lower relative increase found for the analysis based on the GSW data.

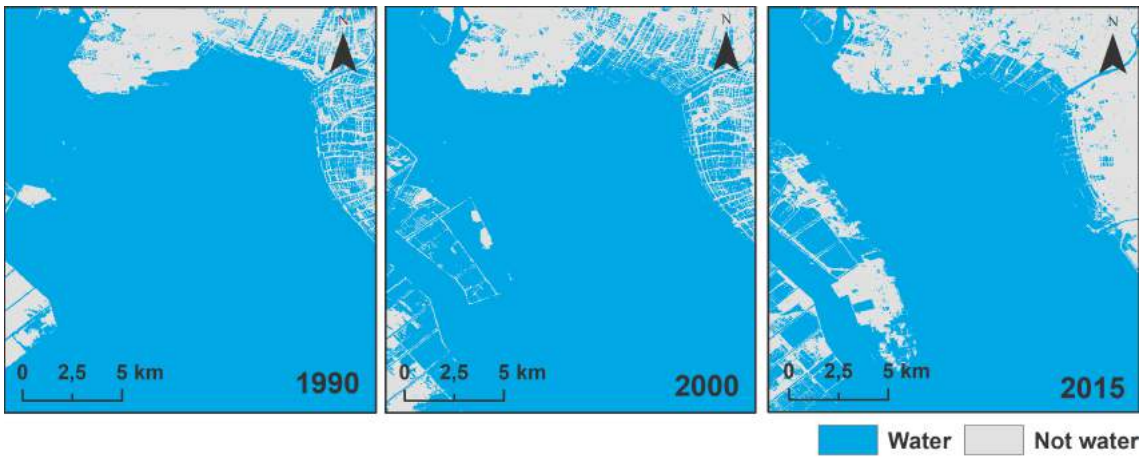

Figure A.19: Natural waters turned into aquaculture in the PRD. Especially the coastal regions are very dynamic and aquaculture ponds have been installed in the sea.

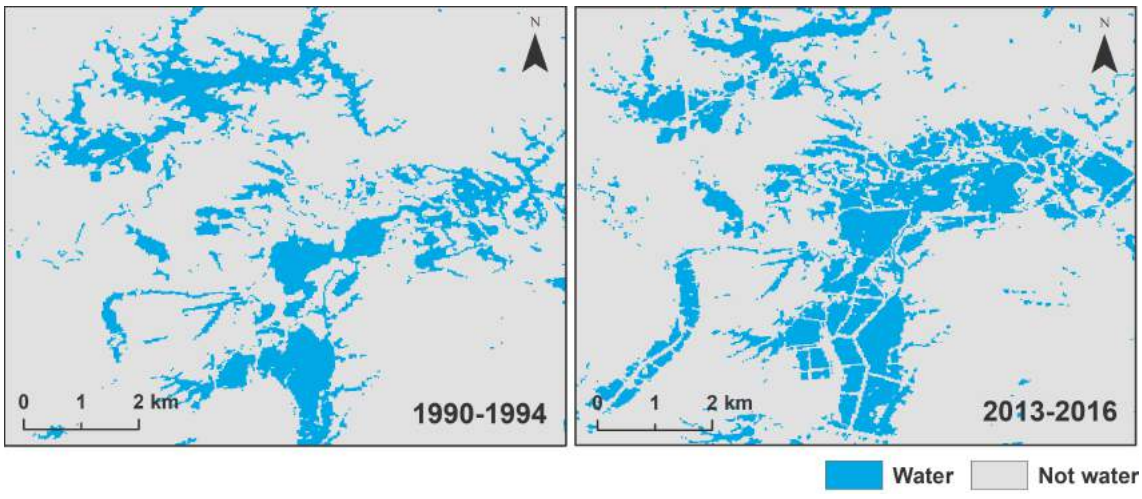

Figure A.20: Natural waters turned into aquaculture in the RRD. This example shows inland water bodies which have been turned into aquaculture ponds.